

***DETERMINATION OF EARTH'S TRANSIENT AND EQUILIBRIUM CLIMATE
SENSITIVITIES FROM OBSERVATIONS OVER THE TWENTIETH CENTURY:
STRONG DEPENDENCE ON ASSUMED FORCING***

S. E. Schwartz

Submitted to
Surveys in Geophys.

July 2011

Atmospheric Sciences Division/Environmental Sciences Dept.

Brookhaven National Laboratory

**U.S. Department of Energy
Office of Science**

Notice: This manuscript has been authored by employees of Brookhaven Science Associates, LLC under Contract No. DE-AC02-98CH10886 with the U.S. Department of Energy. The publisher by accepting the manuscript for publication acknowledges that the United States Government retains a non-exclusive, paid-up, irrevocable, world-wide license to publish or reproduce the published form of this manuscript, or allow others to do so, for United States Government purposes.

This preprint is intended for publication in a journal or proceedings. Since changes may be made before publication, it may not be cited or reproduced without the author's permission.

DISCLAIMER

This report was prepared as an account of work sponsored by an agency of the United States Government. Neither the United States Government nor any agency thereof, nor any of their employees, nor any of their contractors, subcontractors, or their employees, makes any warranty, express or implied, or assumes any legal liability or responsibility for the accuracy, completeness, or any third party's use or the results of such use of any information, apparatus, product, or process disclosed, or represents that its use would not infringe privately owned rights. Reference herein to any specific commercial product, process, or service by trade name, trademark, manufacturer, or otherwise, does not necessarily constitute or imply its endorsement, recommendation, or favoring by the United States Government or any agency thereof or its contractors or subcontractors. The views and opinions of authors expressed herein do not necessarily state or reflect those of the United States Government or any agency thereof.

Determination of Earth's transient and equilibrium climate sensitivities from observations over the twentieth century: Strong dependence on assumed forcing

Stephen E. Schwartz

Atmospheric Sciences Division, Brookhaven National Laboratory

Upton NY 11973

01-631-344-3100

01-631-344-2887

ses@bnl.gov

<http://www.ecd.bnl.gov/steve>

Surveys in Geophysics (special issue)
Space Sciences Series of ISSI (Vol. TBD)
[Submitted 2011-07-20]

Abstract

Relations among observed changes in global mean surface temperature, ocean heat content, ocean heating rate, and calculated radiative forcing, all as a function of time over the twentieth century, that are based on a two-compartment energy balance model, are used to determine key properties of Earth's climate system. The increase in heat content of the upper ocean, obtained as the average of several recent compilations, is found to be linearly related to the increase in global temperature over the period 1965-2009; the slope, augmented to account for additional heat sinks, which is an effective heat capacity of the upper, short-time-constant compartment of the climate system, is $21.8 \pm 2.1 \text{ W yr m}^{-2} \text{ K}^{-1}$ (one-sigma), equivalent to the heat capacity of 170 m of seawater (for the entire planet) or 240 m for the world ocean. The rate of planetary heat uptake, determined from the time derivative of ocean heat content, is found to be proportional to the increase in global temperature relative to the beginning of the twentieth century with proportionality coefficient $1.05 \pm 0.06 \text{ W m}^{-2} \text{ K}^{-1}$. Transient and equilibrium climate sensitivity were examined for six published data sets of forcing mainly by incremental greenhouse gases and aerosols over the twentieth century as calculated by radiation transfer models; these forcings ranged from 1.1 to 2.1 W m^{-2} , spanning much of the range encompassed by the 2007 assessment of the Intergovernmental Panel on Climate Change (IPCC). For five of the six forcing data sets a rather robust linear proportionality obtains between the observed increase in global temperature and the forcing, allowing transient sensitivity to be determined as the slope. Equilibrium sensitivities determined by two methods that account for the rate of planetary heat uptake range from 0.24 to 0.75 K $(\text{W m}^{-2})^{-1}$ (CO_2 doubling temperature 0.88 to 2.75 K), less than, to well less than, the IPCC central value and estimated uncertainty range, and strongly anticorrelated with the forcing used to determine the sensitivities. Transient sensitivities, relevant to climate change on the multidecadal time scale, are lower still, 0.19 – 0.42 K $(\text{W m}^{-2})^{-1}$. Values of the time constant characterizing the response of the upper ocean component of the climate system to perturbations range from 4 to 9 years, in broad agreement with other recent estimates, and much shorter than the time constant for thermal equilibration of the deep ocean, ca. 500 years.

Keywords: *Climate sensitivity; Forcing; Global mean surface temperature; Heat capacity; Time constant*

1. Introduction

The response of the Earth climate system to perturbations in the radiation budget is central to the physiology of the planet. Knowledge of this response is essential to societal decisions about limiting emissions of greenhouse gases in order not to commit the planet to unacceptable climate change. A key measure of the susceptibility of climate to such change is the equilibrium sensitivity, the equilibrium change in global mean near-surface air temperature (GMST) that would result from a sustained change in global net absorbed radiation (forcing, normalized to this forcing¹. Numerous climate model studies have indicated that this change in GMST is relatively insensitive to nature of the radiative change and as well that other changes in climate scale with changes in GMST. The equilibrium sensitivity is a quintessentially important property of Earth's climate system which is the objective of much of the research endeavor directed to understanding Earth's climate and its response to perturbations. Frequently the equilibrium climate sensitivity is expressed as a "CO₂ doubling temperature" $\Delta T_{2\times}$, the amount by which GMST would ultimately increase in response to a sustained doubling of atmospheric CO₂. $\Delta T_{2\times}$ is related to the equilibrium sensitivity by $\Delta T_{2\times} = F_{2\times} S$, where $F_{2\times}$ is the forcing that would result from a doubling of CO₂, approximately 3.7 W m⁻² (Myhre, 1998; IPCC, 2007). The equilibrium sensitivity (or equivalently $\Delta T_{2\times}$) is quite uncertain; the best estimate for $\Delta T_{2\times}$ given by the 2007 assessment report of the Intergovernmental Panel on Climate Change (IPCC, 2007) is 3 K, with an uncertainty range (central 66% of the probability distribution function) 2 to 4.5 K (relative range 83%). This uncertainty greatly limits understanding of climate change over the industrial period and precludes effective planning of energy futures (Schwartz et al, 2010).

¹ For reasons having to do with stratospheric adjustment that occurs rapidly (months) following an increase CO₂, which has traditionally been used as a benchmark forcing in model studies of climate sensitivity, the forcing pertinent to climate change and to determination of climate sensitivity has long been considered to be the change in net absorbed radiation at the tropopause. Increasingly, however, it is becoming recognized (e.g., Gregory and Forster, 2008) that the pertinent measure of forcing is the change in net radiation at the top of the atmosphere, as it is this change that affects the global energy balance.

Broadly speaking, approaches to determining the climate sensitivity can be distinguished as model-based and observation-based. Model based determination is generally taken to mean through the use of general circulation models (GCMs) of the Earth climate system. Such models are capable of

imposing a forcing of known magnitude on the climate system and determining the sensitivity from the climate system response, accounting for the departure of the system from equilibrium through the net heating rate of the planet (Forster and Taylor, 2006). Observationally based determination would generally require knowledge of both the forcing that is thought to have induced a change in GMST over a given period of time and the resultant temperature change attributable to that forcing, necessitating confident attribution of the response to the forcing. In principle this approach might be based on equilibrium change in radiation and GMST over a long period of time (up to and including differences between glacial ice ages and the present temperate period) or might be based on shorter-term forcing and response (e.g., volcanic aerosols, or over the industrial period with ramped forcing) with some means of accounting for the observed response being only a fraction of the equilibrium response. An alternative approach of determining climate sensitivity as the quotient of the climate system time constant upon the effective heat capacity (Schwartz, 2007; Andrews and Allen, 2008, Held, 2010), which is attractive as it does not require knowledge of forcing, remains controversial (Foster, 2008; Knutti, 2008; Schwartz, 2008a; Kirk-Davidoff, 2009).

An important early effort to infer climate sensitivity from observations (Gregory et al. 2002) concluded that uncertainty in forcing over the twentieth century, attributable mainly to uncertainty in forcing by aerosols, admitted a wide range of climate sensitivity, with 90% confidence interval of $\Delta T_{2\times}$ ranging from 1.6 K to infinity. Another important prior study is the examination of what is denoted here as the transient climate sensitivity from the slope of a regression of observed change in global mean temperature over the latter part of the twentieth century against modeled forcing over that period (Gregory and Forster, 2008). An important theoretical and climate-model-based analysis is that of Gregory (2000), who emphasized the role of heat transfer from the rapidly responding upper ocean compartment of the climate system to the deep ocean and thereby serving as an effective sink of heat from the upper compartment in limiting the rate of increase of global temperature, a point that has been elaborated on by Baker and Roe (2009) and Held et al., (2010). An alternative approach (Forster and Gregory, 2006; Murphy et al., 2009) has reported climate sensitivity inferred from observations over shorter periods of time, over which the change in forcing, and hence the associated uncertainty, were arguably less, together with changes in GMST and inferences of the energy imbalance from satellite measurements and/or changes in ocean heat content.

Here I examine relations among observed changes in global mean surface temperature, and ocean heat content, ocean heating rate, together with several model-based estimates of forcing, all as a function of time over the twentieth century to adduce the effective heat capacity of the upper ocean pertinent to climate change over this period, the heat exchange coefficient between the upper ocean and the deep ocean, transient and equilibrium climate sensitivities, and the time constants for response of the climate system to perturbations. The effective heat capacity and heat exchange coefficient so adduced are independent of assumptions about radiative forcing over this period, but the sensitivities and the response time constants are strongly dependent on the radiative forcing employed in the analysis.

2. Theory

The energy conservation equation for Earth's climate system is

$$\frac{dH}{dt} \equiv N = Q - E. \quad (1)$$

Here H is the global heat content anomaly (relative to an arbitrary year or period); $N \equiv dH / dt$ is the net heat flux into planet; Q is the absorbed solar energy, and E is the emitted longwave flux. Other sources or sinks of energy are negligible (Schwartz, 2008b; Pilewskie, 2011). In considering the consequences of a forcing, i.e., a radiative flux perturbation imposed on the climate system, it is useful to consider a situation in which a forcing is imposed on a system that is initially at radiative steady state (commonly denoted “equilibrium”) in which the net flux is equal to zero: $N_0 = 0$. Whether such a situation is ever achieved is perhaps a question of threshold and averaging time. For example fluctuations in the solar constant on an eleven-year cycle would set a floor on the steadiness of the initial state; similarly there are inevitably fluctuations arising from internal variability such as ENSO and from occasional forcing by aerosols from eruptive volcanos. In this steady-state situation the emitted longwave radiation, averaged over the planet and over a sufficiently long time (greater than a year, to average over seasonal variation) is very closely equal to the absorbed solar radiation: $E_0 = Q_0$. Upon application of a perturbation in radiative flux, or forcing, F the net flux into the climate system is altered, a positive forcing corresponding to an increase in heat content of the system (positive N).

$$N = F + Q - E \quad (2)$$

Upon application of this forcing, taken as positive, the system responds by an increase in GMST; this increase in temperature induces a change in the absorbed and/or emitted power. To first order in temperature change ΔT

$$N = F + Q_0 - E_0 + \frac{\partial(Q - E)}{\partial T} \Delta T = F - \lambda \Delta T \quad (3)$$

where the partial derivative denotes the changes in Q and E due to the response of the climate system to the change in temperature (but explicitly not including the change in net flux that is the forcing itself). Here

$$\lambda \equiv -\frac{\partial(Q - E)}{\partial T} \quad (4)$$

is the equilibrium climate sensitivity coefficient, the sign of which is chosen to make λ a positive quantity. For a positive forcing, initially the net flux into the planet N is increased by the magnitude of the forcing; as the temperature increases in response to this forcing the value of N decreases as the system approaches a new steady state (commonly denoted "equilibrium"), as illustrated schematically in Figure 1 for a hypothetical step-function forcing. For this constant forcing, as the new equilibrium is reached, N once again approaches zero, and ΔT approaches $\lambda^{-1}F$. The inverse of λ , $S_{\text{eq}} \equiv \lambda^{-1}$ is denoted the "equilibrium climate sensitivity", the amount by which GMST would change in response to a sustained forcing, normalized to the value of the forcing. Commonly, especially in the context of examining the consequences of alternative scenarios of future CO₂ emissions, the equilibrium sensitivity is expressed as the amount by which the global mean surface temperature would increase in response to a sustained doubling of atmospheric CO₂, $\Delta T_{2\times}$; within the linear range of the relation between increase in GMST and forcing, $\Delta T_{2\times}$ is equal to $F_{2\times} S_{\text{eq}}$, where $F_{2\times}$ is the forcing corresponding to a doubling of CO₂, which is about 3 - 4 W m⁻². $F_{2\times}$ is commonly (Myhre, 1998; IPCC, 2007) given as 3.71 W m⁻², although that precision is hardly justified by the accuracy with which $F_{2\times}$ is known for the actual climate system (Stevens and Schwartz, 2011) or represented in current climate models (Webb et al., 2006, Forster and Taylor, 2006) because of issues involving radiation transfer, especially in cloudy atmospheres (Collins et al., 2006), and short-term responses of clouds to changes in CO₂ (Andrews et al., 2009). In this paper the primary results for sensitivity are presented in systematic units, K (W m⁻²)⁻¹, with values of $\Delta T_{2\times}$, evaluated with $F_{2\times} = 3.71 \text{ W m}^{-2}$, presented for convenience.

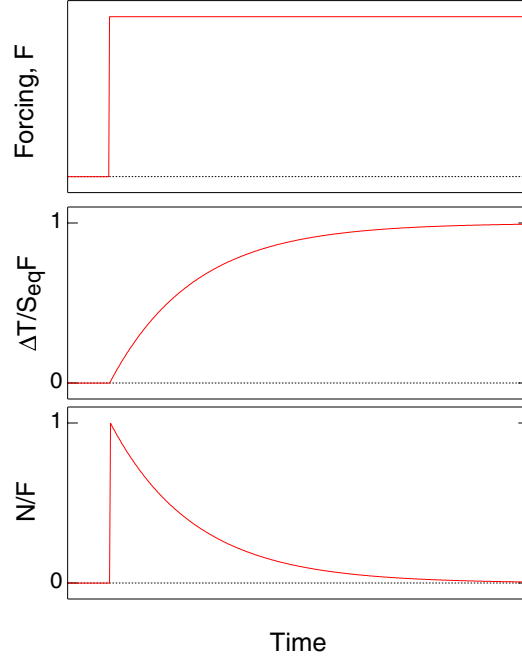


Figure 1. Schematic of forcing temperature anomaly ΔT , and net flux N versus time following onset of step-function forcing. Initially following the onset of the forcing the net flux is equal to the forcing. At long time ΔT approaches $S_{eq}F$, the product of the equilibrium sensitivity times the forcing, and the rate of uptake of energy by the climate system N returns to zero.

Equation 3 suggests a direct proportionality (constant ratio) between $\Delta T(t)$ and $F(t) - N(t)$, where the dependence of all quantities on secular time t , as would result from temporally variable forcing, is explicitly noted,

$$F(t) - N(t) = \lambda \Delta T(t), \quad (5)$$

or in terms of the sensitivity

$$\Delta T(t) = S_{eq}(F(t) - N(t)), \quad (6)$$

from which it is seen that a plot of $\Delta T(t)$ vs. $F(t) - N(t)$ would be expected to be linear through the origin with slope S_{eq} , provided both $F(t)$ and $\Delta T(t)$ are measured from the same initial steady-state condition. This relation suggests that S_{eq} can be determined as the slope of a graph of $\Delta T(t)$ vs. $F(t) - N(t)$. To distinguish this method of determining S_{eq} from a second method described below I denote this approach the " $F - N$ method".

Numerous investigators have suggested the possibility that the time-dependent temperature change $\Delta T(t)$ is proportional to the forcing even under the circumstance that a new steady-state has not been

reached. Such a situation might arise when the forcing is increasing at a constant rate. This situation is closely approximated in the commonly conducted model experiments in which CO₂ mixing ratio is increased at a constant percentage rate (e.g., 1% yr⁻¹, compounded), which leads to exponential growth of CO₂ mixing ratio, and in turn, because of the approximately logarithmic dependence of forcing on CO₂ mixing ratio, results in an approximately constant rate of increase of forcing. This expectation has led to the concept of a transient climate sensitivity, $S_{tr} = \Delta T(t) / F(t)$ that exhibits little time dependence, at least after short-lived transients have died out. A further objective of this study is to examine the transient sensitivity based on current estimates of time-dependent forcing and observed change in GMST over the twentieth century.

A second consideration is assessment of the hypothesis that the rate of heating of the planet is proportional to ΔT ; such an assumption seems plausible based on a simple two-compartment model of the climate system as illustrated in Figure 2 (*cf.* also Gregory, 2000; Held et al., 2010). Here the upper compartment, which consists of the atmosphere and the upper ocean, is strongly coupled to the incoming solar irradiance and the outgoing thermal infrared radiation at the top of the atmosphere. A positive forcing applied to this compartment induces a warming of this compartment that induces a heat flow into the larger-heat-capacity deep ocean. The time required for the lower compartment to respond to any forcing is much greater than that for the upper compartment. For the heat capacity of the upper compartment estimated from the depth of the mixed layer (ca., 100 m) and that for the lower compartment from the average depth of the world ocean (ca 3800 m) the ratio of the heat capacities would be approximately 40. Hence it is reasonable to posit that during the time the system is being externally forced and for some time thereafter the temperature change of the lower compartment is much less than that of the low-heat-capacity, rapidly accommodating upper compartment and hence that the rate of heat transport from the upper reservoir to the lower reservoir is proportional to the increase in temperature of the upper compartment; *cf.* also Forster and Taylor (2006); Boer et al., (2007); Gregory and Forster (2008),

$$N(t) = \kappa \Delta T(t). \quad (7)$$

The heat exchange coefficient κ , like the equilibrium climate sensitivity, is an intrinsic property of Earth's climate system.

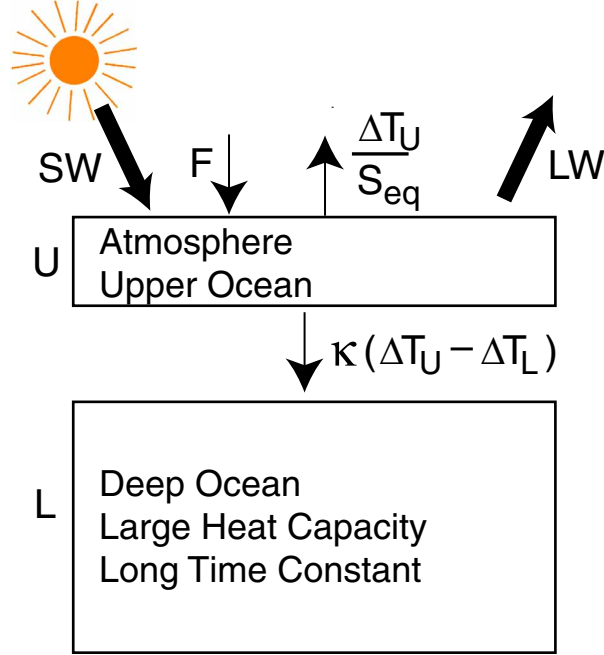


Figure 2. Two-compartment model for Earth's climate system, consisting of upper reservoir U with small heat capacity and short time constant for reaching steady state following a perturbation, and lower reservoir L with large heat capacity and long time constant for reaching steady state. Thick arrows denote initial shortwave (SW) and longwave (LW) fluxes, and thin arrows denote perturbations: forcing F and resultant heat flows, a change in net top-of-atmosphere irradiance given by the time-dependent forcing minus the time-dependent change in temperature T_U of the upper compartment U upon the equilibrium sensitivity S_{eq} , and a heat flux from the upper compartment to the lower compartment L given by the heat exchange coefficient κ times the difference in temperature changes between the upper and lower compartments.

The two-compartment model (Gregory, 2000; Knutti et al., 2008, Schwartz, 2008a; Held et al., 2010) exhibits two time constants (inverses of the eigenvalues) that characterize the rate of relaxation of the system to a perturbation. Specializing to the situation in which the lower compartment is much larger than the upper compartment, and has much greater heat capacity C_L than that of the upper compartment C_U , yields (Held, 2010) for the two time constants (to first order in C_U/C_L)

$$\tau_s = \frac{C_U}{\kappa + \lambda} \quad \tau_l = C_L \left(\frac{1}{\lambda} + \frac{1}{\kappa} \right), \quad (8)$$

where the subscripts s and l denote short and long time constants characterizing the response of the upper ocean to radiative forcings and the ultimate approach to the new steady state involving change in heat content of the entire deep ocean, respectively. Note that the short time constant pertinent to

the upper ocean compartment is related to the heat capacity of this compartment by the sum of the inverse equilibrium sensitivity λ and the heat exchange coefficient κ . Determination of the equilibrium sensitivity $S_{\text{eq}} \equiv \lambda^{-1}$ and the heat exchange coefficient κ together with knowledge of the heat capacities of the compartments permits determination of the time constants, or vice versa.

The two-compartment model suggests that the heat capacities of the two components of the climate system may be identified as follows. The heat capacity of the large compartment is that of the global ocean, which may be evaluated as the volume of the global ocean times the volumetric heat capacity seawater. For the fractional area of Earth covered by ocean as 0.71 and the average depth of the world ocean taken as 3800 m, the average depth per area of the entire planet is 2700 m. For the volumetric heat capacity of seawater taken as $4.0 \times 10^6 \text{ J m}^{-3} \text{ K}^{-1}$, the areal heat capacity $C_L = 1.1 \times 10^{10} \text{ J m}^{-2} \text{ K}^{-1}$. For climate change considerations it is convenient to express this heat capacity in the unit $\text{W yr m}^{-2} \text{ K}^{-1}$, yielding $C_L = 340 \text{ W yr m}^{-2} \text{ K}^{-1}$. The effective heat capacity of the upper compartment of the climate system that is coupled to the change in global temperature may be obtained (Schwartz, 2007) from the relation between the observed change in global heat content H and the observed change in global temperature. As shown previously (Schwartz, 2007) and updated below for the further available measurements, a linear relation is obtained between ocean heat content anomaly and global temperature anomaly allowing evaluation of the effective ocean heat capacity to be evaluated as the slope of a plot of the two quantities. This heat capacity is then augmented to account for other heat sinks (heating of the atmosphere and upper solid earth; melting of ice) to yield the heat capacity of the upper compartment C_U . As determined below, this quantity is more than an order of magnitude less than C_L , consistent with the two compartment model outlined above and with the expressions for the time constants given in Eq (8).

A proportionality between global heating rate and the increase in surface temperature would result in a further proportionality, between the time-dependent increase in surface temperature $\Delta T(t)$ and the time dependent forcing $F(t)$: From (5) and (7)

$$F(t) = (\kappa + \lambda)\Delta T(t) \quad (9)$$

Eq (9) suggests a so-called transient sensitivity analogous to the equilibrium sensitivity, $S_{\text{tr}} \equiv (\kappa + \lambda)^{-1}$ that relates the time dependent increase in surface temperature to the time-dependent forcing,

$$\Delta T(t) = S_{\text{tr}} F(t), \quad (10)$$

which implies that a graph of $\Delta T(t)$ vs. $F(t)$ would likewise be expected to be linear through the origin, in this case with slope S_{tr} . This transient climate sensitivity is the same quantity as that determined from observed temperature change and modeled forcing by Gregory and Forster (2008), except that their quantity is referred to the forcing of doubled CO_2 and is thus greater by a factor of 3.7. Identification of S_{tr} with $(\kappa + \lambda)^{-1}$ together with Eq 8a yields the equation, $S_{\text{tr}} = \tau_s / C_U$ relating the transient climate sensitivity, the effective heat capacity of the climate system, and the time constant for response of the climate system to forcings employed by Schwartz (2007) to infer this sensitivity from the heat capacity and the time constant inferred from autocorrelation of fluctuations in GMST.

The approach of the present study is to examine the several proportionalities: $\Delta H(t)$ vs. $\Delta T(t)$, slope, C_U ; $N(t)$ vs. $\Delta T(t)$, slope κ ; $\Delta T(t)$ vs. $F(t)$, slope S_{tr} ; $\Delta T(t)$ vs. $F(t) - N(t)$, slope S_{eq} , using observations of temperature change and heating rate over the twentieth century and estimates of the forcing over this period. Note that (except for the relation between ΔH and ΔT) each of these several relations is a proportionality; that is, a linear relation with zero intercept. The order of the relation indicates the dependent and independent variables, respectively, under the expectation that the temperature change depends on the forcing but that the heat content and heating rate depend on the temperature change. The relation between S_{eq} and S_{tr} ,

$$S_{\text{eq}} = \frac{1}{S_{\text{tr}}^{-1} - \kappa}, \quad (11)$$

leads to a second method of estimating of S_{eq} based on the heat exchange coefficient κ rather than the individual measurements of heating rate $N(t)$; I denote this method the " κ method".

A further important quantity that can be determined by this analysis is the fraction of the equilibrium increase in global temperature that would result from the imposed forcing up to a given time that has been realized by the increase in global temperature at that time, f_{obs} , which given by the ratio of the transient and equilibrium sensitivities:

$$f_{\text{obs}} \equiv \frac{\Delta T_{\text{obs}}}{\Delta T_{\text{eq}}} = \frac{S_{\text{eq}}}{S_{\text{tr}}} = 1 - \kappa S_{\text{tr}} \quad (12)$$

This quantity depends on the transient sensitivity, which in turn depends on the forcing, but for the situation that ΔT is proportional to the forcing is independent of the time elapsed subsequent to the onset of the forcing.

The estimates of climate sensitivities and other quantities obtained in this way are not wholly observationally based but are hybrids between observationally and model-based estimates of these quantities, as the time-dependent forcing is not directly observed but is based on radiative transfer calculations for measured or modeled changes in atmospheric composition. Carrying out examination of these quantities for a suite of forcing estimates allows examination of consistency of the model and the estimates of forcing, by a linear proportionality of temperature change and forcing, and of the dependence of the inferred climate sensitivities on the forcing.

This entire analysis is rooted in the forcing-response model of climate change; that is, that the change in global mean temperature is a consequence only of forcing under the assumption that forcings are fungible; that is, that GMST response is independent of the nature and geographical distribution of the forcing. This assumption sees considerable justification based on climate model calculations, albeit with some variation in efficacy of different forcings (e.g. Hansen et al., 1997; Joshi et al., 2003; Kloster et al., 2010).

3. Results and interpretation

3.1 Global heating rate and surface temperature

The major accessible reservoir for storing planetary heat energy is the world ocean on account of the high specific heat of water and the relatively rapid rate of heat exchange within the ocean by virtue of turbulent mixing and circulations on a variety of scales. The basis for determination of the global heating rate rests on the data base of historical measurements of ocean temperature as a function of location, depth, and time. These temperature measurements are converted into heat content anomaly as a function of time (relative to a specified base period) via the heat capacity of ocean water and integration over the volume of the world ocean. The measurement data base extends back to about 1950, but the early measurements are sparse, and there remain questions about the accuracy of the primary measurements and the coherence of measurements by different types of sounding instruments and platforms, which have changed over time. The measurements have been analyzed by several groups, with broad agreement but significant differences based on

differences of approach and assumptions about measurement techniques; for reviews see Palmer et al (2010) and Lyman (2011). A composite of the data compilations for anomaly of heat content of the world ocean from the surface to 700 m is shown in Figure 3; most of the increase in ocean heat content is due to warming within the top 700 m, and most of that within the top 300 m (Levitus et al., 2005). Also shown in the figure is the average of the data obtained by the several groups; in order not to bias the average at times where different data sets contributed to the average, all anomalies were computed relative to the years 1993-2002, for which period all data sets are represented.

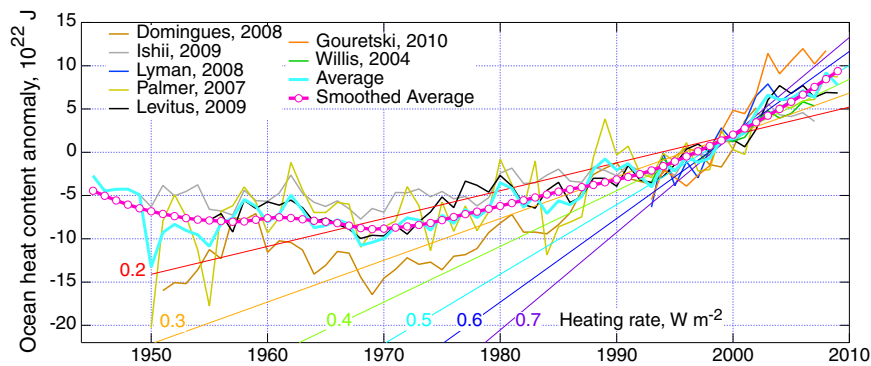


Figure 3. Recent evaluations of ocean heat content anomaly (0-700 m), relative to 1993-2002. Also shown are the average of the several estimates and a LOWESS smoothed curve based on the average. Slopes of lines show heating rate referred to Earth surface area. Data from <http://www.ncdc.noaa.gov/bams-state-of-the-climate/2009-time-series/ohc> (retrieved November 5, 2010) which gives the citations to the publications; data have been updated from the indicated publications by Palmer et al (2010).

Determining the heating rate of the global ocean requires taking a derivative of the heat content; this is complicated by the temporal variability of the data. This variability may be noise associated with the measurements and/or may be a manifestation of actual variability of ocean heat content, a consequence perhaps of internal climate variability such as ENSO or of change in heating rate due to variability in forcing, such as by volcanic aerosol forcing. In order to smooth the data to permit taking the time derivative the LOWESS algorithm (locally weighted scatterplot smoothing; Cleveland and Devlin, 1988) was used to construct a smooth curve that retained the slow temporal variability of the data (magenta curve in Figure 3); the heating rate of the upper ocean was obtained as the derivative of this quantity. A sense of the magnitude of the slope is provided by auxiliary lines drawn on the figure whose slopes correspond to the heating rates indicated, in units of watts per square meter, expressed relative to the total Earth surface area ($5.1 \times 10^{14} \text{ m}^2$), not just the area

of the world ocean. There is indication that since 1970 the slope has been increasing from perhaps 0.3 W m^{-2} to perhaps 0.6 W m^{-2} .

Obtaining the total global heating rate requires estimating other heat sinks in addition to that of the upper ocean. The additional heating from 700 m to 3 km was estimated (Levitus et al., 2005) to be about 30% of that from the surface to 700 m. Other contributions to incremental global heat content, mainly heating of the atmosphere and the land surface and melting of ice, are estimated by Levitus et al. to contribute in the aggregate about 19% additional heating to that of the oceans. The total global heating rate was thus obtained from that of the upper ocean by accounting for heating of the deep ocean (a factor of 1.3) and other heat sinks, a further factor of 1.19. The rate of global heating so obtained is shown as a function of time in Figure 4. Prior to about 1970 the heating rate exhibited fairly large fluctuations and indication even of negative values (net cooling of the planet); these fluctuations may be due to sampling or measurement issues or may reflect actual changes in global heat content. Subsequent to about 1970 the rate of change of global heat content has been consistently positive, albeit not monotonically increasing until after about 1992. Although this variable pattern may again be a consequence of sampling or measurement issues, that possibility seems increasingly unlikely in the later time frame on account of the increase in number and quality of the data and the general tightness of the several compilations of the ocean heat content data. In further support of this argument is the general agreement of the increase in heating rate N with the increase in GMST over the entire time period from about 1960 to the present shown in the time series in Figure 4.

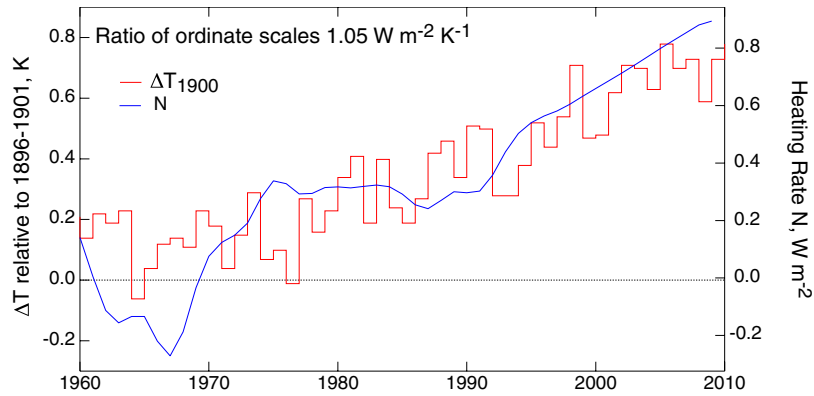


Figure 4. Global mean surface temperature anomaly relative to 1896-1901 ΔT_{1900} (left axis), evaluated from the Goddard Institute for Space Studies (GISS) Combined Land-Surface Air and Sea-Surface Water Temperature Anomalies (Land-Ocean Temperature Index, LOTI) <http://data.giss.nasa.gov/gistemp/tabledata/GLB.Ts+dSST.txt>, (Hansen et al., 2010) and global heating rate N (right axis) evaluated as derivative of smoothed average ocean heat content anomaly shown in Figure 3, augmented to account for deep ocean heating and other heat sinks as described in text, and expressed per area of the planet. Ordinate axes are scaled by the slope of regression forced through the origin (Figure 5).

The relation between global heating rate and global mean surface temperature anomaly (Eq. 7) is examined further in Figure 5, in which the heating rate is plotted against global temperature anomaly relative to 1900, ΔT_{1900} . For the fit restricted to the data from 1965 to the present the regression line has an intercept quite close to zero, $-0.02 \pm 0.05 \text{ W m}^{-2}$ (1 sigma, calculated under assumption of zero autocorrelation), and the regression fit constrained to pass through the origin accounts for virtually the same fraction of the variance (68%) as the two parameter fit; that is, the heating rate is proportional to the increase in surface temperature relative to 1896-1901. This finding is relatively insensitive to the start date of the correlation, with intercept ranging from $-0.06 \pm 0.05 \text{ W m}^{-2}$ (start date 1960) to $+0.10 \pm 0.04 \text{ W m}^{-2}$ (start date 1970), so the finding of linear proportionality (zero intercept) would appear to be robust. The corresponding values for the slope of the regression forced through the origin are 1.02 ± 0.06 , 1.05 ± 0.06 , and $1.07 \pm 0.05 \text{ W m}^{-2} \text{ K}^{-1}$ for start date 1960, 1965, and 1970, respectively. The rather tight correlation between global heating rate (as inferred from heating rate of the upper ocean) and the increase in global temperature relative to the beginning of the twentieth century supports the hypothesis that this heating rate is proportional to global mean surface temperature anomaly, Eq (7), with heat exchange coefficient $\kappa = 1.05 \pm 0.06 \text{ W m}^{-2} \text{ K}^{-1}$. The proportionality of heating rate and global temperature, independently determined, is consistent with the two-compartment model with a much greater heat

capacity in the lower compartment, as described above and supports the utility of using the time-dependent heating rate and/or the regression slope in examination of the relation between global temperature change and various estimates of forcing over the twentieth century.

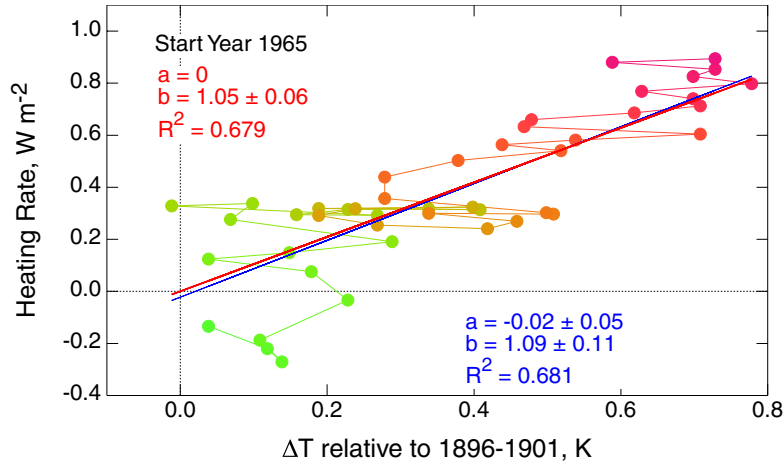


Figure 5. Global heating rate (evaluated as derivative of smoothed average ocean heat content anomaly shown in Figure 3, augmented to account for deep ocean heating and other heat sinks as described in text. and expressed per area of planet) vs. global mean surface temperature anomaly relative to 1896-1901 ΔT_{1900} . Fits to data in the form $dH/dt = a + b\Delta T$ are evaluated for data from 1965 through 2009, with and without constraining regression line to pass through origin; uncertainties in regression coefficients are standard error, calculated under assumption of no autocorrelation. Also indicated as R^2 is fraction of variance in the original data accounted for by the regression. Colors on data points denote date from 1965 (green) to 2009 (red).

3.2 Heat capacity of the upper compartment

The effective areal heat capacity of the portion of the climate system that is actively coupled to the change in global temperature C_U is evaluated from the dependence of the change in ocean heat content on the change in global temperature. As seen in Figure 6, a linear relation is exhibited between the areal heat content anomaly of the upper ocean (to 700 m) and the surface temperature anomaly; the fit was restricted to the data subsequent to 1965, consistent with the analysis for heating rate, but the slope for the entire data set (subsequent to 1945) differed negligibly. The slope of this plot, $14.1 \pm 1.0 \text{ W yr m}^{-2} \text{ K}^{-1}$, represents an effective areal heat capacity of the upper ocean. This effective heat capacity is well less the actual areal heat capacity of seawater to this depth, evaluated as the fractional area of the world ocean 0.71, times the volumetric heat capacity of seawater, $4.0 \times 10^6 \text{ J m}^{-3} \text{ K}^{-1}$, times the depth, 700 m, and expressed in the same units, $63 \text{ W yr m}^{-2} \text{ K}^{-1}$, indicative of the fact that seawater to this depth is not in thermal equilibrium with the increasing

global temperature but is substantially lagging the increase in temperature. Accounting for heating of the ocean deeper than 700 m adds another 30% to this effective heat capacity, yielding $18.3 \text{ W yr m}^{-2} \text{ K}^{-1}$. An alternative way of looking at this result is that this heat capacity corresponds to a hypothetical depth of seawater in thermal equilibrium with the surface temperature, 170 m (for the entire planet) or 240 m for ocean fractional area of 0.71. Finally, accounting for heat sinks in the climate system (air, solid earth, melting of ice) adds a further 19% to the effective heat capacity, yielding $21.8 \pm 2.1 \text{ W yr m}^{-2} \text{ K}^{-1}$, where the uncertainty is a 1-sigma estimate that takes into account the uncertainty in the slope together with estimated uncertainties (25%) in the two augmentations.

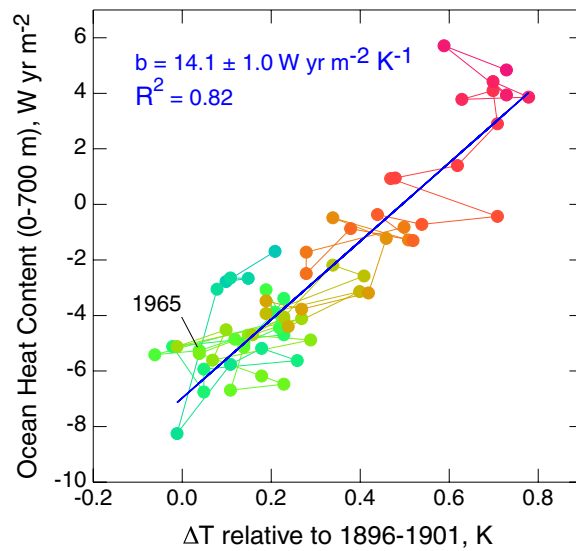


Figure 6. Heat content anomaly of the world ocean (from surface to 700 m, expressed per area of the planet) vs. global mean surface temperature anomaly relative to 1896-1901 ΔT_{1900} . Fit to data in the form $dH/dt = a + b\Delta T$ is evaluated for data from 1965 through 2009; uncertainty in regression slope is standard error, neglecting autocorrelation. Also indicated as R^2 is fraction of variance in the original data accounted for by the regression. Colors on data points denote date from 1945 (light blue) to 2009 (red).

3.3 Forcing

The observationally based determination of climate sensitivity rests on knowledge of climate forcing over the instrumental record. Knowledge of this time-dependent forcing is required also in climate model calculations over the twentieth century. Two approaches have been taken in climate modeling studies to determine the forcing. The forcing may be specified as an input to the model based on measured or modeled changes in atmospheric composition and other radiation influencing

quantities. Alternatively the atmospheric substances influencing radiation in the model are themselves modeled within the climate model and the resulting changes in radiation are calculated within the climate model. The latter approach is increasingly being taken by various modeling groups (Lohmann et al, 2010). As a consequence it seems to be difficult to extract the forcing from climate model runs of the twentieth century. An examination of the literature revealed only a limited number of forcing data sets that were suitable for the present study. In addition to anthropogenic gases and aerosols, whose forcings are to be calculated, modeling the twentieth century requires representation of natural forcings by changes in solar irradiance and, importantly, forcing by stratospheric aerosols that result from eruptive volcanoes. Volcanic eruptions in the twentieth century have resulted in several instances of short-duration forcing, the magnitudes of which are substantial in the context of anthropogenic forcing, and which are manifested in the record of GMST. The several explicitly calculated time series of forcing over the twentieth century available from the literature are summarized in Table 1. In addition to the data sets examined here Forster and Taylor (2006) have presented forcing data sets inferred from the increase in GMST in AR4 model runs over the twentieth century together with the transient sensitivity of these models determined from model runs with 1% per year increment CO₂, for which the forcing is known. The approach appears to yield a fairly accurate estimate of the time-dependent forcing as shown by comparison with forcing data sets employed in the GISS (Goddard Institute for Space Studies; Hansen et al., 2005) and MIROC (Model for Interdisciplinary Research On Climate; Takemura, 2006) model studies for which forcings were explicitly calculated. This method was subsequently applied to determine the forcing time series over the twentieth century in the Hadley Centre model (Jones et al., 2010). In view of the indirect means of inferring the forcing these forcing data sets were not examined in the present study, although it might provide further insight to extend this approach to forcing time series so obtained.

Table 1. Forcing data sets examined in this study.

Data Set	Reference and data source	Forcing, 1900-1990, $W m^{-2}$
GISS, Goddard Institute for Space Studies	Hansen et al., 2005, Figure 1a; http://data.giss.nasa.gov/modelforce/RadF.txt	1.6
RCP - Representative Concentration Pathways	Meinshausen et al., 2010; http://www.pik-potsdam.de/~mmalte/rcps/data/20THCENTURY_MIDYEAR_RADFORCING.xls	1.6
GFDL, Geophysical Fluid Dynamics Laboratory	Held et al., 2010 Figure 2; numerical file provided by I. Held, 2011.	1.9
MIROC, Model for Interdisciplinary Research On Climate	Takemura et al., 2006, Figure 2a; numerical file provided by T. Takemura, 2011.	1.1
PCM, Parallel Climate Model, National Center for Atmospheric Research	Meehl et al., 2003, Figure 1; numerical file provided by G. Strand, 2011.	2.1
Myhre	Myhre et al., 2001, Figure 1; http://folk.uio.no/gunnarmy/data/rf_time/rf_time.dat	1.0

The forcing data set employed in climate model studies by the investigators at the Goddard Institute for Space Studies (GISS; Hansen et al., 2005), Figure 7, is illustrative of current forcing data sets. Shown in the figure are forcings attributable to the several changes in atmospheric composition and surface properties over the twentieth century. Attention is called first to the forcing by the well mixed greenhouse gases (GHGs), a positive (warming) forcing which exhibits a relatively smooth increase over the time period. Similarly the negative (cooling) forcing of reflective aerosols and the aerosol indirect effect both exhibit relatively smooth increases in magnitude with similar time history to the GHG forcing. Negative forcing by volcanic stratospheric aerosols in contrast is highly irregular, exhibiting large values immediately following volcanic eruptions, but decaying to near zero over the course of a few years. Other forcings are relatively small, even in the aggregate. Solar forcing exhibits a cyclical behavior with a roughly 11-year period, indicative of the change in the solar constant associated with the sunspot cycle. Forcings by black carbon from incomplete combustion may be thought of as offsetting part of the negative aerosol cooling forcing. There are minor contributions from the increase in tropospheric and stratospheric ozone, and the increase in stratospheric water vapor resulting from the increase in tropospheric methane, some of which makes its way into the stratosphere and is oxidized there. Changes in surface albedo from black carbon on snow and from land use changes also make minor contributions. The total forcing, evaluated as the

sum of the several components, exhibits a general positive trend over the period but is punctuated by the large, short-duration negative forcings by volcanic stratospheric aerosols, such that the total forcing can, even in the latter part of the twentieth century, exhibit brief excursions into negative values (relative to 1880) before returning to the gradual positive forcing.

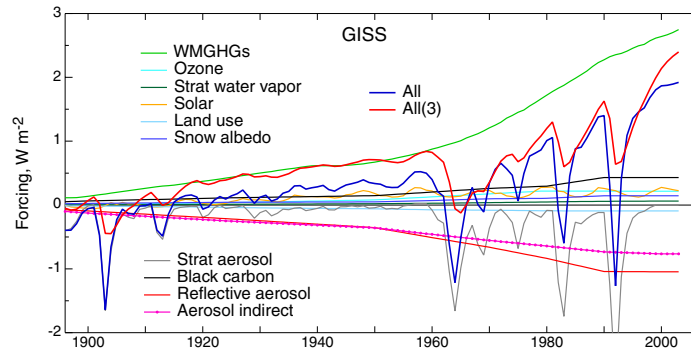


Figure 7. Global mean forcings (relative to 1880) as employed in the Goddard Institute for Space Studies (GISS) climate model (Hansen et al., 2005; <http://data.giss.nasa.gov/modelforce/RadF.txt>). WMGHGs, well mixed greenhouse gases. "All" denotes the total forcing, the sum of the individual forcings, and "All(3)" denotes that forcing convolved with the function $\exp(-t/3)/3$.

In order to relate forcing to temperature change it is necessary to take into account the damping effect of global surface temperature on the rapid impulses in forcing associated with volcanic eruptions. The approach I have taken is to impose a damping on the forcing by convolving the total forcing from the several data sets with a decaying exponential function having a 3-year time constant, $\exp(-t/3)/3$, where t is time in years. As expected this damped forcing, also shown in Figure 7, exhibits reduced magnitude but extended duration of the stratospheric volcanic aerosol forcing. To assess the suitability of this approach I compared the time series of the damped forcing with that of observed global mean surface temperature anomaly, Figure 8. It is seen that the two time series exhibit qualitatively similar behavior in the response to the impulses due to volcanic aerosols, suggesting that the 3-year exponential function is doing a reasonable job of accounting for the time lag of global temperature to the volcanic forcing, especially during the latter half of the twentieth century during which the volcanic aerosol forcings are perhaps better characterized. The 3-year time constant is similar to that found in analysis of GCM data by Held et al (2010), 4 ± 1 years but is somewhat shorter than that determined from analysis of autocorrelation of global mean temperature data, 6-11 years (Scafetta, 2008; Schwartz, 2008a). A fairly short damping time

constant is desired so as to minimize any artificial lag of the more slowly varying forcings arising from the gradual increases in greenhouse gases and aerosols.

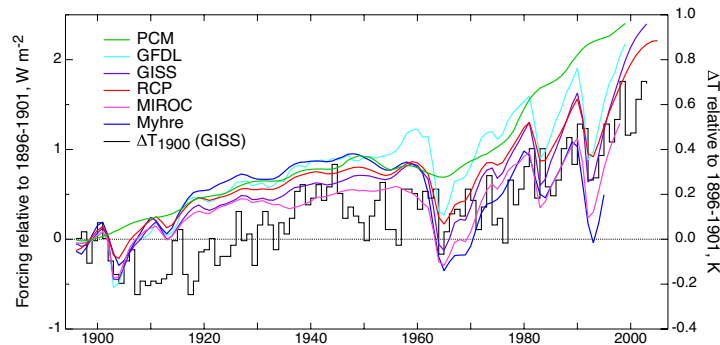


Figure 8. Total forcings from the several forcing data series examined in this study, convolved with the function $\exp(-t/3)/3$. Also shown for comparison is the time series of global mean surface temperature anomaly as tabulated by the Goddard Institute for Space Studies (GISS; Combined Land-Surface Air and Sea-Surface Water Temperature Anomalies, LOTI; <http://data.giss.nasa.gov/gistemp/taledata/GLB.Ts+dSST.txt>)

Also shown in Figure 8 are the time series for the several other forcing data sets examined in this study, similarly convolved with the 3-year exponential decay function. With the exception of the PCM data series, which did not include volcanic aerosol forcing, all the data series exhibit qualitatively similar behavior over the time period, and all exhibit an increase in forcing over the twentieth century, reflecting the dominant contribution of forcing by GHGs. However closer comparison of the several data sets, Figure 9, shows considerable differences among them. Examination of the scatter plots shows strong correlation of the GISS, RCP, GFDL, and MIROC forcings but with offsets from the diagonal, which would indicate perfect agreement. Not surprisingly the PCM forcing data set exhibits poorer correlation because of volcanic aerosol forcing not being included in that data set; this is manifested by downward departure of the other data sets from the PCM data set in "streamers" associated with periods of volcanic aerosol forcing. The data set of Myhre et al. (2001) exhibits rather poor correlation with the other forcing data sets.

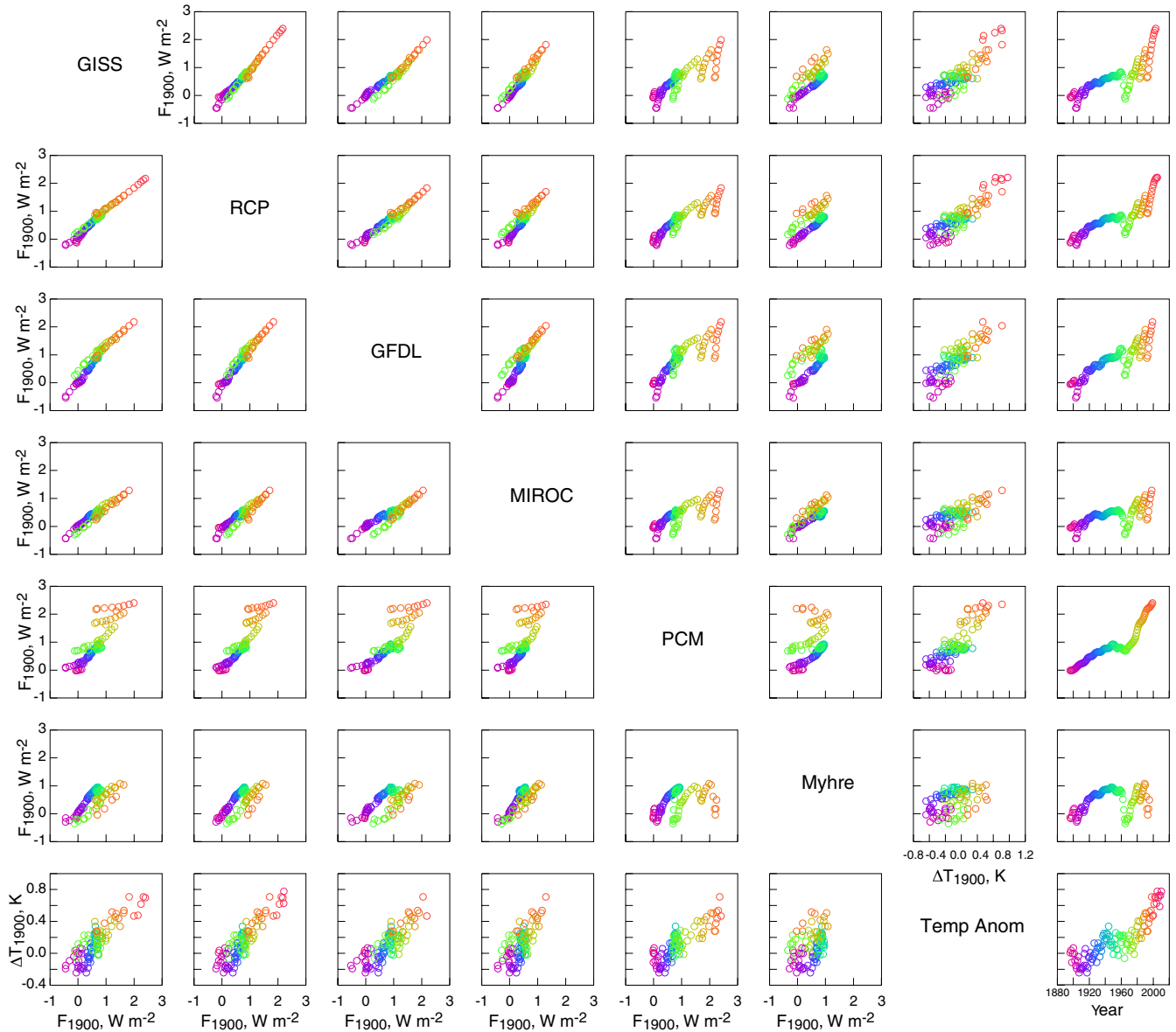


Figure 9. Scatterplot matrix of the several forcings (relative to 1896-1901) employed in this study and also global mean surface temperature anomaly (also relative to 1896-1901). The column and row headings of the several data sets are given along the trace of the matrix, and each graph represents a scatter plot of the quantity identified by the row heading on the y axis versus the quantity identified by the column heading on the x axis. All of the forcings are shown on the same scale; perfect agreement between two different forcing data sets would be manifested by all data lying along the diagonal. Similarly a linear dependence of temperature anomaly on forcing would be manifested by a linear array of the data points. The right hand column gives the time series of each of the forcings and temperature anomaly. The color coding reflects the date (violet, 1896 to red, 2009).

3.4 Correlation of temperature anomaly and forcing

As the intent of this study is to examine the relation of the change in GMST to radiative forcing over the twentieth century, for which the forcing and temperature data are available, it was considered essential that the forcing and temperature anomaly time series be defined relative to values of these quantities in a common time period at the beginning of the century. It was considered desirable as well that this time period be one of relative constancy in both quantities. Examination of the data indicated that the time period 1896-1901 inclusive met these criteria; recovery from the large negative excursion due to the eruption of Krakatoa in 1883 is largely complete by this time. As there is a negative excursion in both forcing and temperature from further volcanic activity commencing in 1902, that year is excluded from the base period. Examination of Figure 8 shows that the variation in the several data sets over the base period 1896-1901 is quite small relative to variation over the data set as a whole, lending support to the choice of the average over this time period as the reference value for both forcing and temperature change over the twentieth century.

Attention is called also to the large range of forcing over the full span of the time series. To some extent this is a consequence of the differing end dates of the time series; it might be argued that the time series of Myhre et al., which terminates in 1995, is not fully recovered from the Pinatubo event. However even so, in 1990, prior to the Pinatubo eruption, the forcing in the six data sets, Table 1, exhibits a span of a factor of 2 and a relative range (range divided by median) of 69%. This range is characteristic of, but well less than, the uncertainty in total forcing over the twentieth century, as given in the IPCC Fourth Assessment Report (2007), best estimate 1.6 W m^{-2} ; 90% confidence range ($0.6 - 2.4 \text{ W m}^{-2}$), or relative range 113%. A range in forcing will inevitably lead to a corresponding range in any assessment of climate sensitivity that is obtained using the several values of forcing together with the time series of observed surface temperature. A key objective of this study is to assess the range in transient and equilibrium sensitivities that results from the range of forcing estimates.

The relation between surface temperature anomaly and forcing was examined by means of graphs of surface temperature anomaly relative to the 1896-1901 base period versus forcing relative to the same period, Figure 10; these graphs are the same as in the bottom row of Figure 9. Note that the y -data of all graphs are the same, the observed temperature change, but it is the x -data, the forcings

adduced by the several modeling groups that differ among the figures. As the hypothesis under examination is that surface temperature has increased in response to the applied forcing, the forcing is taken as the independent (known) variable in the regressions, and the regression coefficients are obtained by minimization of the squares of the residuals of temperature about the regression line. In this analysis the regressions are restricted to the forcing and temperature data for 1965 and beyond, consistent with the start date of the regression for heating rate, but both the forcing and temperature anomaly data are referenced to the common base period, 1896-1901, which, as indicated above, would seem to be a period of little departure of either from the preindustrial situation. However the entire data sets for forcing and temperature from 1896 to the end of the several forcing data sets are shown, and it would seem from inspection of the graphs that for most of the forcing data sets the entire time series is well represented by a linearly proportional relation. In the regressions a rather robust linear proportionality is exhibited for most of the forcing data sets between surface temperature and forcing, albeit with different slopes. The fraction of the variance in the temperature data accounted for by the regression forced through the origin is over 50% for four of the six forcing data sets. For most of the data sets the intercept is near zero, and constraining the regression line to pass through the origin results in little decrease in the fraction of the variance in the data accounted for by the regression, denoted R^2 in the figures and in Table 2. (For the 2-parameter fits R^2 is equal to the square of the Pearson product-moment regression coefficient, as usual; for the 1-parameter fits the quantity denoted R^2 is explicitly evaluated from the residuals; the value of R^2 for the 2-parameter fit necessarily exceeds that for the 1-parameter fit.) A high correlation with zero intercept, that is, temperature anomaly proportional to forcing, is consistent with a planetary heating rate N that is likewise proportional to the temperature increase (Eqs. 9, 10). The sole exception among the forcing data sets examined to the linear proportionality between surface temperature and forcing is for the forcing data set of Myhre et al. (2001), which exhibits poor correlation and for which constraining the regression line to pass through the origin results in a variance about the regression line that actually exceeds the variance in the temperature data themselves. Thus the Myhre forcing data set would seem entirely inconsistent with a linear proportionality between observed temperature change and forcing.

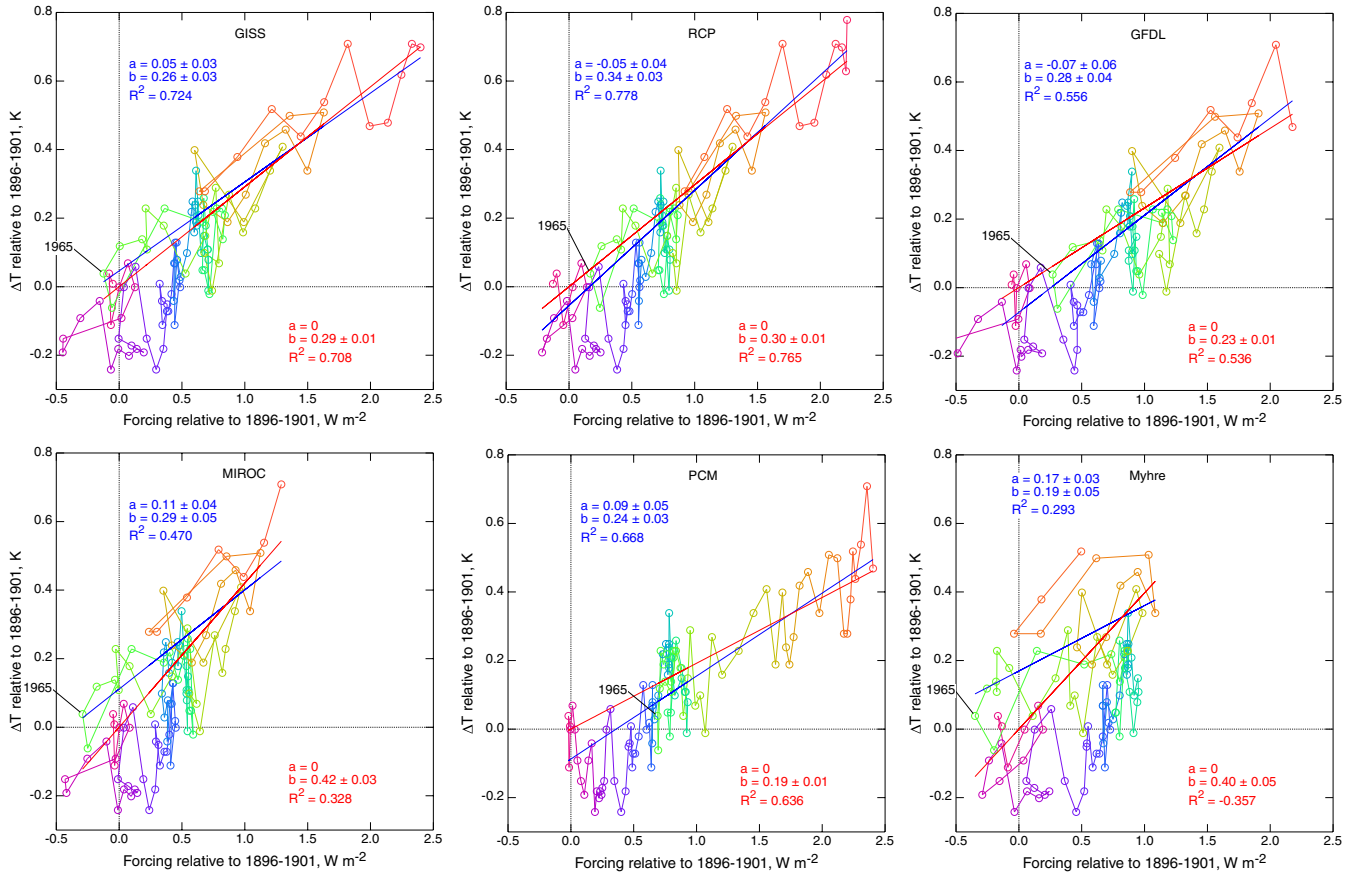


Figure 10. Surface temperature anomaly (relative to 1896-1901) versus total forcings from the several forcing data series examined in this study, as convolved with the function $\exp(-t/3)/3$. Fits to data in the form $\Delta T = a + bF$ from 1965 (indicated) to the ends of the several forcing data series are ordinary linear least squares, blue, and least squares but with a held equal to 0, red. Also indicated as R^2 is fraction of variance in the original data accounted for by the regression; negative value indicates that variance in the residuals about the regression exceeds that in the temperature data themselves. The color coding reflects the date (violet, 1896 to red, 2009).

Table 2. Equilibrium climate sensitivity S_{eq} and transient sensitivity S_{tr} and other quantities determined for the several forcing data sets examined in this study. S_{tr} was evaluated as coefficient of proportionality between temperature anomaly and forcing. S_{eq} was determined by two methods: directly as coefficient of proportionality between temperature anomaly and forcing minus planetary heating rate ($F - N$ method), and via S_{tr} , accounting for the planetary heating rate, as $S_{\text{eq}} = (S_{\text{tr}}^{-1} - \kappa)^{-1}$ (Eq 10) where κ is the coefficient of proportionality between heating rate and temperature anomaly (κ method). R^2 denotes fraction of variance in temperature anomaly data set accounted for by the linear regression with zero intercept. Uncertainties denote 1-sigma estimates inferred from least-squares fits (neglecting autocorrelation), suitably propagated for derived quantities. Relative range denotes range divided by median.

Method	Quantity	Unit	Forcing Data Set						Relative range
			GISS	RCP	GFDL	MIROC	PCM	Myhre	
	$F(1900-1990)$	W m^{-2}	1.6	1.6	1.9	1.1	2.1	1.0	0.69
$F - N$	S_{eq}	$\text{K (W m}^{-2}\text{)}^{-1}$	0.41	0.42	0.29	--	0.23	--	0.54
	$\sigma(S_{\text{eq}})$	$\text{K (W m}^{-2}\text{)}^{-1}$	0.02	0.02	0.02	0.07	0.01		
	R^2		0.66	0.68	0.38	-0.15	0.63	-0.22	
	$\Delta T_{2\times}$	K	1.52	1.55	1.07	--	0.85		0.54
	$\sigma(\Delta T_{2\times})$	K	0.07	0.07	0.07	0.26	0.04		
κ	S_{tr}	$\text{K (W m}^{-2}\text{)}^{-1}$	0.29	0.30	0.23	0.42	0.19	--	0.79
	$\sigma(S_{\text{tr}})$	$\text{K (W m}^{-2}\text{)}^{-1}$	0.01	0.01	0.01	0.03	0.01		
	R^2		0.71	0.77	0.54	0.33	0.64	-0.36	
	S_{eq}	$\text{K (W m}^{-2}\text{)}^{-1}$	0.42	0.44	0.30	0.75	0.24		1.23
	$\sigma(S_{\text{eq}})$	$\text{K (W m}^{-2}\text{)}^{-1}$	0.02	0.02	0.02	0.10	0.02		
	$\Delta T_{2\times}$	K	1.54	1.62	1.12	2.78	0.88		
	$\sigma(\Delta T_{2\times})$	K	0.09	0.09	0.07	0.38	0.06		
	τ_s	yr	6.3	6.5	5.0	9.2	4.1		0.79
	$\sigma(\tau_s)$	yr	0.6	0.7	0.5	1.1	0.5		
	η	yr	466	473	427	579	405		0.38
	$\sigma(\eta)$	yr	17	16	18	33	18		
	f_{obs}		0.70	0.69	0.76	0.56	0.80		0.35
	ΔT_{comm}	K	1.01	1.02	0.92	1.25	0.87		0.38

3.5 Determination of equilibrium climate sensitivity by the κ method.

As described above, if the energy imbalance of the planet (net energy flow into the planet) is linearly proportional to the change in temperature, the transient sensitivity (slope of a graph of temperature change vs. forcing, as in Figure 10) would be related (Eq 9) to the geophysical quantities κ and λ as $S_{tr} \equiv (\kappa + \lambda)^{-1}$. Thus, within this model, for κ independently determined from observations of the change in GMST and rate of change of global heat content (Figure 5) it is possible to determine the equilibrium sensitivity as $S_{eq} = (S_{tr}^{-1} - \kappa)^{-1}$. These relations are used to evaluate S_{eq} from the transient sensitivities determined for the several forcing data sets; the results are given in Table 2 as are the corresponding values of the CO₂ doubling temperature evaluated as $\Delta T_{2\times} = F_{2\times} S_{eq}$, where $F_{2\times}$ is the forcing for doubled CO₂, for which the value employed here is 3.71 W m⁻². As is the case with the values of the transient sensitivity, the differences in the values of the equilibrium sensitivity determined for the several forcing data sets are due entirely to differences in the forcing data sets. The relative range of the values of the equilibrium climate sensitivity, 123%, is substantially greater than that in the forcings themselves or in the transient sensitivities because of the subtraction involved in the calculation of S_{eq} .

3.6 Determination of equilibrium climate sensitivity from correlation of temperature change with $F - N$

According to Eq (6) surface temperature anomaly as a function of time would be expected to exhibit a linear proportionality to forcing F minus planetary heating rate N , also both functions of time, with slope equal to the equilibrium sensitivity S_{eq} . This relation was examined by means of graphs of surface temperature anomaly relative to the 1896-1901 base period versus forcing relative to the same period minus heating rate N for the several forcing data sets, Figure 11. In these graphs the time period represented by the data is limited to the period subsequent to 1949, for which heating rate data are available. As the accuracy and representativeness of the ocean heat content data prior to 1965 are questionable, fits to obtain linear regressions were carried out only for the data from 1965 through the ends of the several forcing data sets. As in the plots of temperature change versus forcing, the y-data of all graphs are the same, the observed temperature change, but it is the x-data, the forcings calculated by the several modeling groups minus the planetary heating rate derived from the increase in ocean heat content (which is the same for all the graphs) that differ among the figures; differences in the slopes among the several graphs are thus entirely a consequence of the

differences in the forcing data sets. As the hypothesis is that surface temperature increases in response to the forcing minus the planetary heating rate, the latter is taken as the independent (known) variable in the regressions and the regression coefficients are obtained by minimization of the squares of the residuals of temperature about the regression line.

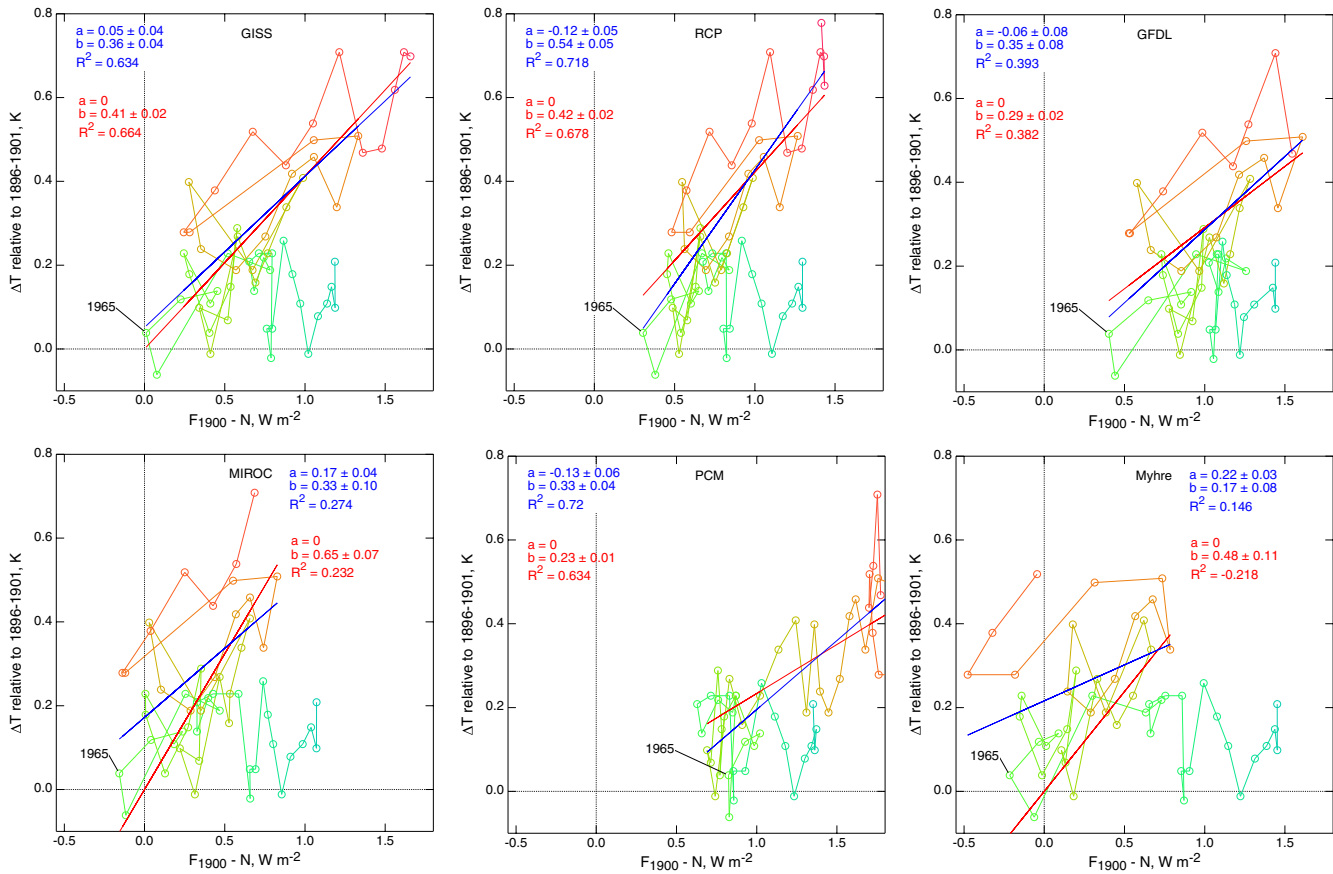


Figure 11. Surface temperature anomaly (relative to 1896-1901) versus $F - N$, where F is total forcings from the several forcing data series examined in this study, as convolved with the function $\exp(-t/3)/3$, and N is planetary heating rate shown in Fig. 4. Data are shown for the entire time period for which ocean heat content data are available, extending to 1949, but regression fits to data in the form $\Delta T = a + b(F - N)$ are limited to the time period from 1965 (indicated) to the ends of the individual forcing data series. Fits are ordinary linear least squares, blue, and least squares but with the intercept a held equal to 0 K, red. Also indicated as R^2 is fraction of variance in the original data accounted for by the regression; negative value indicates that variance in the residuals about the regression exceeds the variance in the temperature data themselves. The color coding reflecting the date (light blue, 1949, to red, 2009), is consistent with the color coding of Figure 9).

Examination of the regression fits presented in Figure 11 between ΔT and $F - N$ (see also Table 2) shows fairly robust correlations, $R^2 > 0.6$, for three (GISS, RCP, and PCM) of the six forcing data sets, with intercepts, corresponding to zero forcing, close to 0 K, and with little decrease in the fraction of the variance accounted for by the regression for the regression line constrained through the origin; such a relation is indicative of a linearly proportional dependence of ΔT on $F - N$ that would be expected for the energy balance model. For the GFDL forcing data a similar linear proportionality is indicated but with considerably reduced R^2 . In all cases the R^2 values are less than that exhibited in the regression of heating rate on surface temperature anomaly, 0.679 (Figure 5), which would seem to indicate that the forcing data introduce additional variance into the relation. For the MIROC and Myhre forcing data sets only a rather small fraction of the variance is accounted for by the regression, and constraining the regression line to pass through the origin at $F = 0$ not only results in a worsening of the fit relative to the 2-parameter fit (as required mathematically) but actually results in the variance about the regression line exceeding the variance characterizing the temperature anomaly data about their mean value; this situation is revealed by a negative value of R^2 , evaluated as the fraction of the variance in the data accounted for by the regression. The departure from linear proportionality between ΔT and $F - N$ for the Myhre et al. and MIROC forcings should not necessarily be taken as implying that the forcing data do not provide an accurate picture of actual forcing of Earth's radiation balance over this time period, but it would certainly seem that these forcing data, together with the observations of increase in temperature and planetary heating rate, are inconsistent with an energy balance model for which the change in net emitted irradiance at the top of the atmosphere is proportional to the increase in surface temperature.

The values of equilibrium sensitivity determined by the $F - N$ method would appear to exhibit a much smaller relative range than those determined by the κ method. However, the difference is due entirely to inclusion of the sensitivity determined with the MIROC forcing data in the set of values of S_{eq} obtained by the κ method, whereas this data set is excluded from the values of S_{eq} obtained by the $F - N$ method because of failure to exhibit a linear regression. If that value of S_{eq} is removed from the set of values obtained by the κ method, the relative range is virtually identical, and indeed the values of S_{eq} by the two methods agree within their one-sigma uncertainties. The identity of the results obtained by the two different methods lends support to the two methods and values obtained.

3.7 Other climate system properties

Determination of the heat capacities of the two compartments of the climate system, the heat exchange coefficient κ , and the transient sensitivity S_{tr} permits determination of the response time constants of the two compartments, Eq 8. In terms of the observationally determined quantities:

$$\tau_s = C_U S_{tr}; \quad \tau_l = \frac{C_L}{(\kappa - S_{tr} \kappa^2)},$$

where for C_L I take the heat capacity of the world ocean given above, $340 \text{ W yr m}^{-2} \text{ K}^{-1}$. The time constants differ for the different forcing data sets because of the dependence of S_{tr} on forcing. For each forcing data set the short and long time constants differ by almost two orders of magnitude, showing the sharp demarcation between the two quantities.

A final key property of interest is the fraction of the equilibrium increase in GMST that would result from a given forcing that is manifested by the increase in GMST at a given time of observation, f_{obs} , Eq (12). Values of f_{obs} given in Table 2 for the several forcing data sets range from 0.56 to 0.80.

4. Discussion

4.1 Heat capacity of the upper compartment of the climate system

The graph of ocean heat content anomaly versus temperature anomaly gives rise, as a slope, to the effective heat capacity of the ocean that is coupled to the climate system, from which the total effective heat capacity of the climate system was obtained by taking into account other sinks of heat in the climate system. The resulting effective heat capacity $21.8 \pm 2.1 \text{ W yr m}^{-2} \text{ K}^{-1}$ is somewhat greater, and is determined with considerably less uncertainty, than the value given by a similar approach by Schwartz (2007), $14 \pm 6 \text{ W yr m}^{-2} \text{ K}^{-1}$, a consequence mainly of improved estimates of ocean heat content anomaly subsequent to the study of Levitus et al. (2005) on which the earlier determination was based. However this uncertainty reflects only scatter about the regression line and does not encompass systematic uncertainty that would result from inadequate sampling and methodological artifacts in the heat content measurements. As determination of this effective heat capacity does not rely on modeled forcings, it is not subject to uncertainties in the forcings and therefore is entirely observationally determined. In an analysis of ocean uptake in climate model runs with the Hadley Centre coupled atmosphere-ocean general circulation model (AOGCM) in

which the CO₂ mixing ratio was increased by 1% yr⁻¹, compounded, Gregory (2000) found an increase in ocean heat content of 7.5×10^{23} J for a temperature increase of 1.8 K, from which a heat capacity of $25.9 \text{ W yr m}^{-2} \text{ K}^{-1}$ may be inferred. Based on climate model studies in which model parameters were allowed to vary, Frame et al. (2005) presented values (0.1 – 2.05) GJ m⁻² K⁻¹ (5–95% confidence), equivalent to (3.2 – 65) W yr m⁻² K⁻¹, a range that encompasses the value obtained here but provides little constraint or insight. Andrews and Allen (2008) present an analysis of this quantity as inferred from studies with coupled AOGCMs yielding a probability distribution function (PDF) for this quantity that peaks at about 0.7 GJ m⁻² K⁻¹ (principal contribution to the PDF between 0.4 and 1.4 G J m⁻² K⁻¹; $22_{-9}^{+22} \text{ W yr m}^{-2} \text{ K}^{-1}$), broadly consistent with the observationally determined heat capacity found here.

Although the analysis of the ocean heat content observations presented here provides a fairly tight constraint on the effective heat capacity, interpretation of the physical meaning of this quantity remains problematic. As the determination is based on the increase in heat content of the entire ocean (and other tightly coupled components of the climate system), the resulting heat capacity is not the heat capacity only of the upper compartment of the ocean. Still, it is certainly not the heat capacity of the deep ocean, which is an order of magnitude greater. Insight into the multiple response times of the climate system from a two-compartment model is provided by Held et al. (2010) and a more thorough interpretation through an upwelling diffusion model is provided by Hoffert et al. (1980). An approach to separating the shallow ocean component from the deep ocean component was advanced by Gregory (2000), who examined temporal autocorrelation of temperature as a function of depth with that in the top ocean layer in output of the Hadley Centre AOGCM, finding a sharp break at about 100 m. It would seem that an observationally based approach such as this might usefully distinguish the upper and lower oceanic components of the actual climate system. In this respect attention is called to a time series of measurements of ocean temperature as a function of depth (surface to 800 m) over a 15 year period (Sutton and Roemmich, 2001) that shows the damping of the amplitude of the seasonal cycle of temperature with depth from about 6 K peak-to-peak at the surface to about 1 K at 150 m, suggesting an observational approach to determining the time-dependent penetration of heat due to a secular change in surface temperature induced by changing atmospheric composition.

4.2 Heat exchange coefficient

The heat exchange coefficient κ , the rate of heat uptake by the planet normalized to the global temperature anomaly was determined as the slope of the linear proportionality between the rate of increase of ocean heat content, evaluated as the time derivative of the ocean heat content, augmented to include estimates of additional heat sinks, and the surface temperature anomaly. This heat exchange coefficient is $1.05 \pm 0.06 \text{ W m}^{-2} \text{ K}^{-1}$, where again the uncertainty reflects the uncertainty in the regression but not systematic errors in the heat content data. For the observed increase in global temperature relative to 1900 $\Delta T_{\text{obs}} = 0.78 \text{ K}$ in 2010 (Hansen et al., 2010, as extended at <http://data.giss.nasa.gov/gistemp/>), this value of κ would indicate a heat flux into the climate system, which is equal to the energy imbalance of the climate system, of 0.82 W m^{-2} . Such an energy imbalance is consistent with the present heating rate shown in Figure 5 (from which it is derived) and with other current observationally based estimates of this quantity (Palmer et al, 2010; Lyman et al., 2011).

As with the effective heat capacity, determination of the heat exchange coefficient is wholly observationally determined. Further, it would seem that this heat exchange coefficient is an intrinsic property of Earth's climate system, rather than a property that is dependent on the nature and/or magnitude of recent forcings. Certainly a proportionality between the rate of heat input into the climate system and the increase in global temperature following imposition of a radiative forcing cannot be maintained indefinitely, as indicated in Figure 1. Nonetheless at least in the early years following the onset of forcing, or perhaps only during situations of continuously increasing forcing, the linear proportionality between the rate of increase of heat content and the temperature anomaly would seem to be a useful means of quantifying the heat input into the climate system and the consequences of the departure from steady state following imposition of the forcing.

Despite considerable interest in the heat exchange coefficient in interpreting climate model calculations (Gregory and Forster, 2008; Dufresne and Bony, 2008), there does not seem to be prior observationally based determination of this quantity. Gregory and Forster determined κ as the slope of a regression of net heat flux into the planet, relative to control runs, against GMST anomaly in the output of 16 AOGCMs that participated in the intercomparison of models over the twentieth century carried out by the IPCC (2007) Fourth Assessment, the same approach as employed here with observation-derived data. For the 16 models examined the mean value of κ was

0.62 ± 0.13 (1 sigma); maximum 0.83; minimum 0.41. It would thus seem that the heat exchange coefficient may be somewhat underestimated in current climate models. For a given equilibrium sensitivity an underestimate would result in the rate of increase in GMST being overestimated in climate model calculations. As the net heat flux is subtractive from the forcing in determining the rate of temperature increase, the magnitude of the overestimate would depend on the forcing. Alternatively knowledge of the heat transfer coefficient might be used to infer the equilibrium sensitivity of a climate model from S_{tr} obtained from the dependence of modeled temperature anomaly on forcing (κ method, Eq 11); as κ is subtractive from S_{tr}^{-1} an erroneously low value of κ would result in an overestimate of S_{eq} , the magnitude of which would depend on the value of S_{tr}^{-1} .

As with the effective heat capacity, it would seem that questions remain regarding the interpretation of this heat flux. Both observationally and from the climate model output, the quantity that is determined is the total net heat flux into the planet, normalized to the global temperature anomaly, whereas the heat flux that is calculated in two compartment models is the heat flux from the upper, short-time-constant compartment to the lower, long-time-constant compartment. As the upper compartment undoubtedly comprises a substantial fraction of the effective heat capacity of the system, it would seem fruitful to more explicitly distinguish between the two compartments in refining these concepts in future work. Nonetheless, it is clear that the net heat flux into the climate system that is subtractive from the applied forcing to yield the equilibrium sensitivity of the climate system, Eq. (6) is the heat flux into the entire climate system. The observationally based finding of a linear proportionality between heat flux and temperature anomaly supports the relation between transient and equilibrium sensitivities, Eq. (11) that can be used to infer the equilibrium sensitivity from the transient sensitivity based on observations (and assumed forcings) or to infer the transient sensitivity from climate model runs that yield the equilibrium sensitivity with slab-ocean models.

4.3 Transient and equilibrium climate sensitivities

This study has examined the relation between observed increase in GMST and forcing, as calculated by several groups, in terms of a two-compartment energy balance model. According to this model a linear proportionality would be expected between the two quantities, the slope of which would be interpreted as a transient climate sensitivity S_{tr} . This expectation is borne out for five of the six forcing data sets examined, for forcing and temperature anomaly over the twentieth century. However the regression slopes (limited to measurements subsequent to 1965) differ for the several

forcing data sets by amounts that substantially exceed the uncertainties in the regression slopes (Table 2) and by amounts that are significant in the context of interpretation of climate change over the twentieth century. Recognition that the planetary heating rate N is subtractive from the forcing F to yield the equilibrium sensitivity S_{eq} suggests a further linear proportionality between GMST anomaly and $F - N$, the proportionality constant being S_{eq} , leading to determination of S_{eq} as this slope, the $F - N$ method. A linear proportionality was found for four of the six data sets examined; again the sensitivities so determined differ by amounts that substantially exceed the uncertainties in the regressions and that are important in the context of understanding climate change. The finding of a linear proportionality between the heating rate and GMST anomaly yielding the heat exchange coefficient κ , permits determination of S_{eq} from S_{tr} , the κ method. This method yielded values of S_{eq} for the five forcing data sets for which it was possible to determine S_{tr} . The values of S_{eq} so determined agreed closely with the values of S_{eq} determined by the $F - N$ method. Here it should be emphasized that the absence of linear proportionality between GMST anomaly and forcing for a single forcing data set of the six examined (that of Myhre et al., 2001) does not demonstrate those forcing data are an inaccurate representation of forcing over the latter part of the twentieth century but only that these forcing data are inconsistent with the energy balance model considered. This inconsistency in a single forcing data set, and more broadly the differences in the sensitivities determined from the several forcing data sets examined, underscore the importance of accurate determination of climate forcing over the twentieth century, especially the latter part of the twentieth century for which ocean heat content data are available, to observational determination of Earth's climate sensitivities.

For the five forcing data sets for which climate sensitivities could be determined, the resulting values, 0.24 to 0.75 K (W m⁻²)⁻¹, corresponding to $\Delta T_{2\times}$ 0.9 – 2.8 K are all less than, and for the most part, well less than, the best estimate and "likely" range² given for this quantity by the 2007 IPCC Assessment, 3 K, (2 – 4.5) K, Figure 12. Of the five forcing data sets, all of which are within the "very likely" range² given for this forcing by the IPCC (2007) Assessment, the only data set for which the equilibrium sensitivity lies within the IPCC "likely" range is the MIROC data set. For each of the other forcing data sets the equilibrium sensitivity is below the lower bound of the "likely" range for this quantity, and indeed is nearly at the limit, or below the limit of the "very likely" range for this quantity, $\Delta T_{2\times} = 1.5$ K. Examination of the relation between the values of S_{tr} and S_{eq} determined by this analysis and the twentieth century climate forcing used to infer the

sensitivity from the observed increase in GMST (Figure 12) shows distinct anticorrelation; that is, a low forcing yields a high sensitivity, and vice versa. Such an anticorrelation, which would be expected for a given increase in GMST has been noted previously in both empirical inference of what now must be recognized as transient climate sensitivity (Schwartz, 2004) and in analysis of the equilibrium sensitivity of climate models (Kiehl, 2007; Knutti, 2008). Of course the equilibrium climate sensitivity, which is a property of Earth's climate system, cannot depend on the forcing. Rather it is the equilibrium climate sensitivities that are inferred from estimates of the forcing that exhibit such dependence. The anticorrelation between equilibrium sensitivity and forcing indicates that the only way that Earth's equilibrium climate sensitivity could be as great as the central value of the IPCC estimate, $\Delta T_{2\times} = 3$ K, would be for the total forcing (recall that the forcing corresponds to the period 1900 – 1990) to be about 0.8 W m^{-2} . Such a low forcing, which is at the low end of the IPCC "very likely" range, would require a rather large negative aerosol forcing to offset the forcing, by the well mixed greenhouse gases, about 2.3 W m^{-2} in 1990; here it must be emphasized that this is not an "inverse" calculation of aerosol forcing, as would be obtained by using a modeled sensitivity, but rather an observational constraint on this forcing together with the best estimate of the equilibrium climate sensitivity given by the IPCC assessment. Extrapolation of the anticorrelation between equilibrium sensitivity and forcing to the entire span of the "very likely" range for the total forcing given by the IPCC 2007 Assessment (0.6 to 2.4 W m^{-2}) yields a range in equilibrium sensitivity $0.07 - 0.91 \text{ K(W m}^{-2})^{-1}$ ($\Delta T_{2\times} 0.26 - 3.4 \text{ K}$), more than an order of magnitude. This wide range of equilibrium climate sensitivity underscores the importance of constraining the forcing if the climate sensitivity is to be determined with accuracy, either observationally or in climate model studies. The analysis also indicates that the observed increase in GMST over the latter part of the twentieth century can be accounted for only by some combination of large (negative) aerosol forcing and/or low climate sensitivity.

² Here the term "likely" is used in the sense of the 2007 IPCC Assessment Report; that is, corresponding to the estimate of the central 66% of the PDF for the quantity. Likewise the term "very likely" is used to denote the estimate of the central 90% of the PDF.

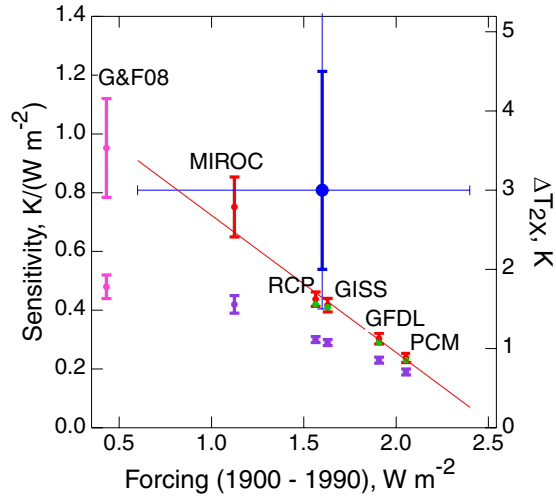


Figure 12. Dependence of transient climate sensitivity S_{tr} , Eq. 10, (purple) and equilibrium climate sensitivity S_{eq} inferred by the $F - N$ method, Eq. 6, (green) and by the κ method, Eq 11, (red) on forcing between 1900 and 1990. Uncertainties in equilibrium sensitivity (shown for the κ method) represent one sigma, estimated by error propagation from the uncertainties in S_{tr} (also shown, one sigma) and κ . Right axis gives equivalent CO_2 doubling temperature evaluated from S_{tr} , or S_{eq} with CO_2 doubling forcing 3.71 W m^{-2} . Also shown (magenta) are S_{tr} , determined by Gregory and Forster (2008) as slope of regression of ΔT observed over the years 1970-2006 against "median" estimates of total forcing by anthropogenic greenhouse gases and aerosols (years strongly affected by volcanic aerosols excluded) and S_{eq} evaluated from that value of S_{tr} using the value of κ determined here, with associated one-sigma uncertainties. Also shown (blue) are best estimates of equilibrium climate sensitivity and anthropogenic forcing (relative to preindustrial) and associated uncertainties as given by the IPCC Fourth Assessment Report (2007); thick uncertainty lines correspond to central 66% of the likelihood function (roughly equivalent to one sigma); thin uncertainty lines denote "very likely" range corresponding to the central 90% of the likelihood function. Red line denotes extrapolation of equilibrium uncertainties to the full "very likely" range of forcing given by the 2007 IPCC assessment.

The most relevant prior study examining the relation of observed temperature change to forcing is that of Gregory and Forster (2008), which presented, for forcing determined by the Hadley Centre climate model, graphs of observed temperature change versus anthropogenic forcing or versus total forcing; years strongly influenced by volcanic emissions were excluded from determination of the regression slope. The transient sensitivity found in that study for temperature change and forcing over the period 1970-2006 is $0.48 \pm 0.04 \text{ K}(\text{W m}^{-2})^{-1}$; the corresponding value of equilibrium sensitivity, evaluated with the value of κ determined here is $0.95 \pm 0.18 \text{ K}(\text{W m}^{-2})^{-1}$ ($\Delta T_{2x} = 3.5 \text{ K}$). These sensitivities are somewhat to substantially greater than the values determined for the forcing data sets examined here, Figure 12. Correspondingly, the forcing data set employed by

Gregory and Forster exhibits a much lower total forcing over the twentieth century, 0.43 W m^{-2} (1900 – 1990) than the several forcing data sets examined here, a value that is less than the lower bound of the "very likely" range for forcing up to 2005 as given by the IPCC, although that gap is closed by the incremental forcing between 1990 and 2005.

4.4 Climate system time constants

Although the time constants for relaxation of perturbations in heat content of the two compartments of the climate system determined by this analysis depend on the magnitudes of the forcings of the several data sets examined, for each of the forcing data sets the time constants associated with the two compartments are clearly separated into a short time constant (median 6.3 yr, range 4.1 – 9.2 yr) and a long time constant (median 470 yr, range 400 – 580 yr). A similar large difference in time constants was noted by Gregory (2000), examining a two-compartment model having parameters chosen to match experiments with the Hadley Centre climate model, who found that the response could be characterized by a short time constant of about 12 yr and as second time constant at least an order of magnitude greater. A large gap in time constants was noted also by Held et al. (2010), in an analysis of the response of the GFDL climate model to step-function changes in forcings, with a short time constant characterizing the transient response of the climate system to an applied forcing and a much longer response time, which they characterize as "centuries or longer" associated with the second, large-heat-capacity compartment of the climate system. Based on an analysis of model runs of two AOGCMs and a model of intermediate complexity run out to equilibrium Jarvis and Li (2011) likewise find two discrete time scales, one of about 20 years and a second of about 700 years. Based on an examination of transient runs across the climate models that participated in the intercomparison reported in the 2007 IPCC Assessment, Lucarini and Ragone (2011) characterized the longer relaxation time as of order 500-700 years. A rapid initial response to forcing that exhibits most of the climate system response to a step function forcing followed by a further response of lower magnitude and long duration is exhibited also in climate model runs presented by Brasseur and Roeckner (2005), Matthews and Caldeira (2007), and Held et al. (2010).

A response of Earth's climate system to perturbations that is characterized by two such widely separated time constants would have important implications for the interpretation of climate change over the past half century during which forcing has likely been systematically increasing. Specifically for such a situation the response of GMST to the forcing would be in rather close

steady state to the forcing, lagging the response given by the transient sensitivity by about one time constant, that is, just a few years. Thus Held et al. (2010) found that the response of the GFDL model to twentieth century forcing is accurately matched by a single-box model with a time constant of 4 yr and a transient sensitivity of $0.43 \text{ K (W m}^{-2}\text{)}^{-1}$. Ultimately, Held et al. find that the heat input into what they term the recalcitrant compartment of the climate system becomes appreciable, but under a situation of continuously increasing forcing, the increase in temperature of this compartment remains a small fraction of that of the short-time-constant compartment. On the time scale certainly of several decades it would seem that the increase in temperature of the deep ocean is insufficient to appreciably diminish the proportionality between temperature anomaly and heat flux. In other words, the response of the climate system to forcing would continue to be given by the transient sensitivity, not the equilibrium sensitivity. This situation would likely continue to hold as temperature anomaly continues to increase. A departure from proportionality between temperature anomaly and heat flux to the long-time-constant compartment might be expected only after some decades of constant forcing, at which point the back flux of heat from the deep ocean compartment to the shallow ocean compartment would begin to become appreciable. Based on these considerations it would seem that the most relevant measure of climate sensitivity for policy purposes is the transient sensitivity, as it is this sensitivity that will govern climate system response to changes in forcing, given that the time constant for the deep ocean compartment to respond to forcings is several centuries.

If the forcing is maintained at a constant value, ultimately, on the time scale of the longer time constant, the global temperature will approach a constant value that is governed by the equilibrium sensitivity, not the transient sensitivity. The difference between the increase in temperature observed at a given time and that which would be expected for the forcing that has given rise to that temperature increase being maintained indefinitely is a committed further temperature increase. The magnitude of this committed further increase is characterized by the fraction of the ultimate increase in temperature that has taken place at a time of observation, f_{obs} , Eq (12), values of which are given in Table 2 for the several forcing data sets. For the observed increase in global temperature in 2010 relative to 1900 $\Delta T_{\text{obs}} = 0.78 \text{ K}$ (Hansen et al., 2010, as extended at <http://data.giss.nasa.gov/gistemp/>), the total committed temperature increase, the increase in GMST relative to 1900 that would be expected if the present forcing for each of the several data sets were maintained indefinitely, ΔT_{comm} , ranges from 0.87 to 1.25 K, and the further committed increase

0.09 to 0.47 K. It should be stressed that these values are dependent on the assumed forcings, but more importantly the calculations assume maintenance of the present forcing indefinitely. Such a situation seems highly unlikely. In an extreme hypothetical case, if emissions of GHGs were to be abruptly halted, such a change in GHG emissions would almost certainly be accompanied by a great reduction in emissions of aerosols and aerosol precursor gases. As the atmospheric residence times of the aerosols are about a week, the (negative) aerosol forcing would immediately be greatly reduced, and the full effect of the GHG forcing would be manifested on the time scale of the short time constant, a few years. This phenomenon has been illustrated in climate model calculations (Brasseur and Roeckner, 2005). Hence the observed fraction of the committed temperature increase calculated under the assumption that the total forcing would be maintained is probably not a meaningful estimate of the actual committed further temperature increase. For present (2010) forcing by the long-lived GHGs taken as 2.8 K and the present ΔT relative to 1900 0.78 K, the committed future increment in GMST for the several forcing data sets ranges from near zero (-0.1 K) to 1.3 K. These estimates are lower to much lower than those obtained for the central value sensitivity of the IPCC 2007 Assessment, 1.5 K, a consequence of the low values of S_{eq} relative to the IPCC best estimate obtained for the several forcing data sets examined.

4.5 Climate sensitivity inferred from climate system time constant as determined by autocorrelation analysis

The value of planetary heat capacity obtained here, together with estimates of the response time of the climate system to perturbations determined from analysis of autocorrelation of global mean surface temperature anomaly, 8.5 ± 2.5 yr (Schwartz, 2007, 2008a; Scafetta, 2008) would give rise (Eq. 8a) to a climate sensitivity, which must now be recognized as a transient sensitivity, evaluated as $S_{tr} = \tau_s / C_U$, $S_{tr} = 0.39 \pm 0.12$ K (W m⁻²)⁻¹; This transient sensitivity in turn, together with the heat exchange coefficient $\kappa = 1.05 \pm 0.06$ W m⁻² K⁻¹ leads (Eq. 11) to an estimate of the equilibrium climate sensitivity $S_{eq} = 0.66 \pm 0.35$ K (W m⁻²)⁻¹ that is determined without any dependence on calculated climate forcing. This value, which lies toward the high end of the range of estimates obtained using estimates of climate forcing, would imply, via the correlation shown in Figure 12, a fairly low total forcing, 1.1 W m⁻². The corresponding equilibrium CO₂ doubling temperature $\Delta T_{2\times} = 2.4 \pm 1.3$ K, albeit somewhat lower than the central value estimated for this quantity by the IPCC (2007) Assessment, 3 K, is well within the "likely" uncertainty range provided by that assessment (2 – 4.5 K).

4.6 What might be wrong with this analysis and how might it be improved?

As emphasized above the present determination of Earth's climate sensitivities and related quantities is a hybrid based on observations of global temperature and ocean heat content and largely model-based calculations of climate forcings. Clearly the several forcings employed in this analysis, which are characteristic of present understanding and uncertainty, cannot all be correct, and the strong dependence of the inferred climate sensitivity to the forcing employed in the analysis underscores the importance of determining forcing with greater accuracy if climate sensitivity is to be determined with confidence (Schwartz 2004; Schwartz et al, 2010). A second source of possible error, affecting all the determinations, is error in planetary heat imbalance inferred here from the rate of uptake of heat by the world ocean. This quantity is subject to uncertainty in the measurements, arising from changes in methods and limited and nonuniform sampling (geographically and as a function of depth) over the period of record, as discussed by Lyman (2011). A greater rate of heat uptake (planetary heat imbalance) would result in a greater inferred equilibrium climate sensitivity than that determined here, and conversely a smaller rate of heat uptake would result in an even lower equilibrium sensitivity, demonstrating the importance of this quantity also in determining climate sensitivity. An inherent limitation to this approach is that it requires determining the rate of heat uptake as a time derivative of the ocean heat content with the attendant requirements on precision and the associated requirement of measurements over an extended time period before the derivative can be inferred with confidence. An alternative approach to determining heat imbalance is through satellite measurements of the net flux at the top of the atmosphere. As discussed by Stevens and Schwartz (2011) an improvement in measurement accuracy of more than an order of magnitude is required to yield an accuracy that is comparable to that of the heat content measurements.

More broadly, the present analysis rests on the whole-Earth forcing and response model and the assumption that changes in heat uptake by forcings that are different in kind and geographical distribution yield the same global average response. Ultimately such a model fails if, for example, there are local feedbacks such as melting of surface ice that amplify the effects of forcings in one location relative to another. Still, the whole-Earth model is attractive in its simplicity and the insights it affords and, at least so far, continues to be useful for these considerations.

5. Summary and conclusions

The present analysis has examined several relations among global mean quantities pertinent to climate change: global heating rate with surface temperature anomaly (slope, heat exchange coefficient); ocean heat content with temperature anomaly (slope, effective heat capacity of the climate system); surface temperature anomaly with forcing over the twentieth century (slope, transient climate sensitivity); and surface temperature anomaly with forcing minus heating rate (slope, equilibrium climate sensitivity). Six published estimates of forcing over the twentieth century were examined. The first two relations, yielding heat exchange coefficient and effective heat capacity, are independent of the forcings and thus do not encompass any model-based uncertainty associated with the forcings, allowing determination of the effective planetary heat capacity and the heat exchange coefficient from measurements of global mean surface temperature anomaly and ocean heat content anomaly over the second half of the twentieth century. All of these relations, and for the relations involving forcings, for most of the forcings examined, exhibited robust linear proportionality (i.e., zero intercept in linear regression; in the case of heat capacity, linear relation), consistent with expectation based on an energy balance model of the climate system. Additionally a second method was applied for evaluating equilibrium climate sensitivity using the heat exchange coefficient that yielded values essentially identical to those of the direct regression.

The results of these correlations are interpreted in terms of a two-compartment energy balance model of Earth's climate system that is characterized by an upper, small-heat-capacity, short-time-constant compartment that corresponds to the atmosphere and upper ocean and a lower, large-heat-capacity, long-time-constant compartment that corresponds to the deep ocean, that is only weakly coupled to the upper compartment. This model leads to a distinction between a transient climate sensitivity, which pertains to the upper compartment, and an equilibrium climate sensitivity, which pertains to the entire climate system including the deep ocean. The analysis leads to estimates of the time constants of the two compartments, which are dependent on the forcing data sets employed, but which are quite separated from one another, 4 to 9 years for the upper compartment, and circa 500 years for the lower compartment. In this situation the response of the climate system to forcings over the twentieth century is governed by the short time-constant of the upper compartment, which is the time constant that governs the relation between forcing and surface temperature anomaly. The proportionality between forcing and temperature anomaly exhibited for all but one of the forcing data sets examined, together with the large separation in time constants, supports the utility of the

transient climate sensitivity, evaluated as the proportionality coefficient of these two quantities as the useful measure of Earth's climate sensitivity for interpretation of climate change over the twentieth century and for informing policy decisions about future emissions.

The analysis presented here, although focusing on observational data, nonetheless rests heavily on the forcings over the twentieth century as calculated by several modeling groups based, ultimately, on measured or modeled changes in atmospheric composition. Of these the forcing due to anthropogenic aerosols is the source of the greatest uncertainty, and it is this uncertainty that is mainly responsible for the differences in forcings over the twentieth century. Confident determination of Earth's climate sensitivities thus remains hostage to accurate determination of these forcings.

Acknowledgment. I thank the several modeling groups for providing the forcing data sets employed in this analysis. An earlier version of this paper was presented at the Workshop on Observing and Modelling Earth's Energy Flows organized and sponsored by the International Space Science Institute in Bern Switzerland, 10-14 January, 2011, and I thank Lennart Bengtsson for his encouragement of this study. This work was supported by the U.S. Department of Energy's Atmospheric System Research Program (Office of Science, OBER) under Contract No. DE-AC02-98CH10886.

References

- Andrews DG, Allen MR (2008) Diagnosis of climate models in terms of transient climate response and feedback response time. *Atmos Sci Lett* 9:7-12. doi:10.1002/asl.163
- Andrews T, Forster PM, Gregory JM (2009) A Surface Energy Perspective on Climate Change. *J Climate* 22 (10):2557–2570
- Baker MB, Roe GH (2009) The Shape of Things to Come: Why Is Climate Change So Predictable? *J Climate* 22:4574-4589. doi:10.1175/2009JCLI2647.1
- Boer GJ, Stowasser M, Hamilton K (2007) Inferring climate sensitivity from volcanic events. *Clim Dyn* 28:481-502. doi:10.1007/s00382-006-0193-x
- Brasseur GP, Roeckner E (2005) Impact of improved air quality on the future evolution of climate. *Geophys Res Lett* 32:L23704. doi:10.1029/2005GL023902
- Cleveland WS, Devlin SJ (1988) Locally-Weighted Regression: An Approach to Regression Analysis by Local Fitting. *Journal of the American Statistical Association* 83 (403):596–610. doi:10.2307/2289282
- Collins WD, Ramaswamy V, Schwarzkopf MD, Sun Y, Portmann RW, Fu Q, Casanova SEB, Defresne J-L, Fillmore DW, Forster PMD, Galin VY, Gohar LK, Ingram WJ, Kratz DP, Lefebvre M-P, Li J, Marquet P, Oinas V, Tsushima T, Uchiyama T, Zhong WY (2006) Radiative forcing by well-mixed greenhouse gases: Estimates from climate models in the IPCC AR4. *J Geophys Res* 111:D14317, doi:10.1029/2005JD006713. doi:doi:10.1029/2005JD006713

- Domingues CM, Church JA, White NJ, Gleckler PJ, Wijffels SE, Barker PM, Dunn JR (2008) Improved estimates of upper-ocean warming and multi-decadal sea-level rise. *Nature* 453:1090-1093. doi:10.1038/nature07080
- Forster PMF, Gregory JM (2006) The climate sensitivity and its components diagnosed from Earth Radiation Budget Data. *J Climate* 19:39-52. doi:10.1175/JCLI3611.1
- Forster PMD, Taylor KE (2006) Climate forcings and climate sensitivities diagnosed from coupled climate model integrations. *J Climate* 19:6181-6194
- Foster G, Annan JD, Schmidt GA, Mann ME (2008) Comment on "Heat capacity, time constant, and sensitivity of Earth's climate system" by S. E. Schwartz. *J Geophys Res* 113:D15102. doi:10.1029/2007JD009373
- Frame DJ, Booth BBB, Kettleborough JA, Stainforth DA, Gregory JM, Collins M, Allen MR (2005) Constraining climate forecasts: The role of prior assumptions. *Geophys Res Lett* 32:L09702, doi:09710.01029/02004GL022241
- Gouretski V, Reseghetti F (2010) On depth and temperature biases in bathythermograph data: development of a new correction scheme based on the analysis of global ocean data. *Deep-Sea Research I* 57:812-833
- Gregory J. M. (2000) Vertical heat transports in the ocean and their effect on time-dependent climate change *Climate Dynamics* 16:501-515
- Gregory JM, Stouffer RJ, Raper SCB, Stott PA, Rayner NA (2002) An Observationally based estimate of the climate sensitivity. *J Climate* 15 (22):3117-3121
- Gregory JM, Forster PM (2008) Transient climate response estimated from radiative forcing and observed temperature change. *J Geophys Res* 113:D23105. doi:10.1029/2008JD010405
- Hansen J, Nazarenko L, Ruedy R, Sato M, Willis J, DelGenio A, Koch D, Lacis A, Lo K, Menon S, Tsvetkov T, Perlwitz J, Russell G, Schmidt GA, Tausnev N (2005) Earth's energy imbalance: Confirmation and implications. *Science* 308:1431-1435, doi:10.1126/science.1110252
- Hansen J, Ruedy R, Sato M, Lo K (2010) Global surface temperature change. *Rev Geophys* 48:RG4004. doi:10.1029/2010RG000345
- Hansen J, Sato M, Ruedy R (1997) Radiative forcing and climate response. *J Geophys Res* 102:6831-6864
- Held IM, Winton M, Takahashi K, Delworth T, Zeng F, Vallis GK (2010) Probing the Fast and Slow Components of Global Warming by Returning Abruptly to Preindustrial Forcing. *J Climate* 23:2418-2427. doi:10.1175/2009JCLI3466.1
- Hoffert MI, Callegari AJ, Hsieh CT (1980) The role of deep sea heat storage in the secular response to climate forcing. *J Geophys Res* 85:6667-6679
- IPCC (2007) *Climate Change 2007: The Physical Science Basis*. In: Solomon S, Qin D, Manning M (eds). Intergovernmental Panel on Climate Change, Geneva, pp <http://ipcc-wg1.ucar.edu/wg1/wg1-report.html>
- Ishii M, Kimoto M (2009) Reevaluation of Historical Ocean Heat Content Variations with Time-varying XBT and MBT depth bias corrections. *J Oceanogr* 65:287-299
- Jarvis A, Li S (2011) The contribution of timescales to the temperature response of climate models. *Climate Dyn* 36: 523-531 doi:10.1007/s00382-010-0753-y

- Joshi M, Shine K, Ponater M, Stuber N, Sausen R, Li L (2003) A comparison of climate response to different radiative forcing in three general circulation models: towards and improved metric of climate change. *Climate Dyn* 20:843-854
- Kiehl JT (2007) Twentieth century climate model response and climate sensitivity. *Geophys Res Lett* 34:L22710. doi:10.1029/2007GL031383
- Kirk-Davidoff DB (2009) On the Diagnosis of Climate Sensitivity Using Observations of Fluctuations. *Atmos Chem Phys* 9:813-822
- Kloster S, Dentener F, Feichter J, Raes F, Lohmann U, Roeckner E, Fischer-Bruns I (2010) A GCM study of future climate response to aerosol pollution reductions. *Climate Dyn* 34:1177–1194. doi:10.1007/s00382-009-0573-0
- Knutti R (2008) Why are climate models reproducing the observed global surface warming so well? *Geophys Res Lett* 35:L18704. doi:10.1029/2008GL034932
- Knutti R, Krähenmann S, Frame DJ, Allen MR (2008) Comment on “Heat capacity, time constant, and sensitivity of Earth’s climate system” by S. E. Schwartz. *J Geophys Res* 113:D15103. doi:10.1029/2007JD009473
- Levitus S, Antonov JI, Boyer TP, Locarnini RA, Garcia HE, Mishonov AV (2009) Global ocean heat content 1955–2008 in light of recently revealed instrumentation problems. *Geophys Res Lett* 36:L07608. doi:10.1029/2008GL037155.
- Lohmann U, Rotstayn L, Storelvmo T, Jones A, Menon S, Quaas J, Ekman AML, Koch D, Ruedy R (2010) Total aerosol effect: radiative forcing or radiative flux perturbation? *Atmos Chem Phys* 10 (7):3235-3246. doi:10.5194/acp-10-3235-2010
- Lucarini V, Ragone F (2011) Energetics of climate models: Net energy balance and meridional enthalpy transport. *Rev Geophys* 49:RG1001. doi:10.1029/2009RG000323
- Lyman JM (2011). *Surveys Geophys* (this issue)
- Lyman JM, Johnson GC (2008) Estimating annual global upper ocean heat content anomalies despite irregular in situ ocean sampling. *J Clim* 21:5629-5641
- Matthews HD, Caldeira K (2007) Transient climate-carbon simulations of planetary geoengineering. *Proc Natl Acad Sci USA* 104:9949-9954
- Meehl GA, Washington WM, Wigley TML, Arblaster JM, Dai A (2003) Solar and Greenhouse Gas Forcing and Climate Response in the Twentieth Century. *JClimate* 16:426-444
- Meinshausen M, Smith S, Calvin K, Daniel JS, Kainuma M, Lamarque J-F, Matsumoto K, Montzka SA, Raper SCB, Riahi K, Thomson AM, Velders GJM, van Vuuren D (2011) The RCP Greenhouse Gas Concentrations and their Extension from 1765 to 2300. *Climatic Change*:submitted
- Murphy DM, Solomon S, Portmann RW, Rosenlof KH, Forster PM, Wong T (2009) An observationally based energy balance for the Earth since 1950. *J Geophys Res* 114:D17107. doi:10.1029/2009JD012105
- Myhre G, Highwood EJ, Shine KP, Stordal F (1998) New estimates of radiative forcing due to well mixed greenhouse gases. *Geophys Res Lett* 25:2715-2718. doi:10.1029/98GL01908

- Myhre G, Myhre A, Stordal F (2001) Historical evolution of radiative forcing of climate. *Atmos Environ* 35:2361-2373
- Palmer MD, Haines K, Tett SFB, Ansell TJ (2007) Isolating the signal of ocean global warming. *Geophys Res Lett* 34:L23610. doi:10.1029/2007GL031712
- Palmer M, Antonov J, Barker P, Bindoff N, Boyer T, Carson M, Domingues C, C. SG, Gleckler P, Good S, Gouretski V, Guinehut S, Haines K, Harrison DE, Ishii M, Johnson G, Levitus S, Lozier S, Lyman J, Meijers A, Schuckmann Kv, Smith D, Wijffels S, Willis J Future observations for monitoring global ocean heat content. In: Hall J, Harrison DE, Stammer D (eds) *Proceedings of the "OceanObs' 09: Sustained Ocean Observations and Information for Society" Conference (Vol. 2), Venice, Italy, 21-25 September 2009, 2010.*
- Pilewskie (2011). *Surveys Geophys (this issue)*
- Schwartz SE (2004) Uncertainty requirements in radiative forcing of climate change. *J Air Waste Manage Assoc* 54:1351-1359
- Schwartz SE (2007) Heat capacity, time constant, and sensitivity of Earth's climate system. *J Geophys Res* 112 (D24):D24S05. doi:10.1029/2007JD008746
- Schwartz SE (2008a) Reply to comments by G. Foster et al., R. Knutti et al., and N. Scafetta on "Heat capacity, time constant, and sensitivity of Earth's climate system". *J Geophys Res* 113:D15105. doi:10.1029/2008JD009872
- Schwartz SE (2008b) Uncertainty in climate sensitivity: Causes, consequences, challenges. *Energy Environ Sci* 1:430-453
- Schwartz SE, Charlson RJ, Kahn RA, Ogren JA, Rodhe H (2010) Why hasn't Earth warmed as much as expected? *J Climate* 23:2453-2464. doi:10.1175/2009JCLI3461.1
- Stevens B, Schwartz S E (2011) *Observing and Modeling Earth's Energy Flows. Surveys Geophys (this issue)*
- Sutton P, Roemmich D (2001) Ocean temperature climate off north-east New Zealand. *New Zealand J Marine Freshwater Res* 35:553-565
- Takemura T, Tsushima Y, Yokohata T, Nozawa T, Nagashima T, Nakajima T (2006) Time evolutions of various radiative forcings for the past 150 years estimated by a general circulation model. *Geophys Res Lett* 33:L19705. doi:10.1029/2006GL026666
- Webb MJ, Senior CA, Sexton DMH, Ingram WJ, Williams KD, Ringer MA, McAvaney BJ, Colman R, Soden BJ, Gudgel R, Knutson T, Emori S, Ogura T, Tsushima Y, Andronova N, Li B, Musat I, Bony S, Taylor KE (2006) On the contribution of local feedback mechanisms to the range of climate sensitivity in two GCM ensembles. *Clim Dyn* 27:17-38, doi:10.1007/s00382-00006-00111-00382. doi:10.1007/s00382-006-0111-2
- Willis JK, Roemmich D, Cornuelle B (2004) Interannual variability in upper ocean heat content, temperature, and thermosteric expansion on global scales. *J Geophys Res* 109:C12036, doi:10.1029/2003JC002260